
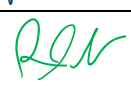






Department Aerospace Engineering
Faculty of Engineering & Architectural Science

Course Code	AER 507
Section	06
Course Title	Materials and Manufacturing
Semester/Year	Fall 2019
Instructor	Jeff Xi
TA	Himanshu Sharma
Project	Glider
Submission Date	November 29 th 2019

Name	Student ID	Signature*
Jann Cristobal	500815181	
Renzo Nicolas	500712830	
Pruthvi Rajput	500828111	
Awon Sharjeel	500811013	

**By signing above you attest that you have contributed to this submission and confirm that all work you have contributed to this submission is your own work. Any suspicion of copying or plagiarism in this work will result in an investigation of Academic Misconduct and may result in a "0" on the work, an "F" in the course, or possibly more severe penalties, as well as a Disciplinary Notice on your academic record under the Student Code of Academic Conduct, which can be found online at:*
<http://www.ryerson.ca/senate/policies/pol60.pdf>

Executive Summary

This report consists of the development and manufacturing of a hand-thrown glider in a competition between several teams, using the materials and tools provided. The wing design was preselected with a NACA M22 airfoil, and each team manufactured and prepared their own wings for the competition. This was done through wrapping fiberglass (10.95 g) and carbon fiber (12.35 g) on a foam skeleton (14 g) and applying an epoxy made of resin (37 g) and hardener (13.2 g). After letting it rest, the untrimmed wing (72.7 g) was trimmed down to the ideal shape (50.2 g). The measured resin to cloth ratio was 2.155 with 12.2%, 7.81% & 79.99% carbon fiber, fiberglass and epoxy volume fractions respectively. The calculated modulus of elasticity of the carbon fiber weft was 15.5 Msi and 960 ksi for the fiberglass weft. It was also determined reaction injection molding is better on an industrial scale as little manual labour is required and the composite comes out stronger. The traditional layup method is reserved for those who have time and lack the resources for RIM or are doing it on a small scale, like this lab. The wing design remained consistent between each team, however the overall glider design varied. Control surfaces were not permitted and the whole glider was required to fit between a 75 cm by 75 cm box. The flight score was determined by the ratio of distance over the glider weight divided by maximum allowable weight of 200g. The fuselage had a NACA 0018 profile to make it streamlined. It was broken into several parts to account for weight and structural integrity. The top of the fuse consisted of hollow shell made of PLA with a thickness of 1.5 mm, whereas the rest of it was polystyrene, as it was lighter and shock absorbent when not hollow. The wing mount consisted of PLA as well. The boom was an 8 mm hollow tube with a thickness of 1mm made of carbon fiber that had its fibers in a single direction. The tail was a conventional tail made of balsa and consisted of lightening holes for weight management. The holes were covered in clear tape and the entire tail was mounted on a brace. The brace consisted of balsa piece and was slotted on the boom with tape holding it in place. The adhesive holding the balsa structures was CA while a lenient amount of tape was used to secure everything else down, alongside tidbits of Velcro. After the many trials and iterations of the glider, it weighed 96 g on competition day and managed to reach 18.6 m with a resulting score of 80.03. This gave it third place overall.

Table of Contents

List of Figures	iii
List of Tables	iii
1. Introduction.....	1
2. Problem Description	3
2.1 Problem Statement	3
2.2 Design Objectives	3
2.2.1 Design Objective List	4
2.3 Design Constraints	5
2.3.1 Competition Rules	5
2.3.2 Wing Dimensions	5
3. Design Concepts	6
3.1 Existing Designs.....	6
3.1.1 Fuselage.....	6
3.1.2 Wing Configurations	8
3.1.3 Tail (T-Tail, Conventional, V-Tail).....	9
3.2 Development of Designs	12
3.2.1 Design 1 – Initial Design Concept (Sketches).....	12
3.2.2 Design 2 – Flight Stability (CATIA’s Inertial Analysis)	13
3.2.3 Design 3 – Mass Optimization, Prototyping and Flight Tests.....	13
3.3 Design Selection.....	15
3.3.1 Pairwise Comparison Chart.....	15
3.3.2 Morphological Chart.....	16
4. Final Design Description	17
4.1 Fuselage.....	17
4.1.1 Design.....	17
4.1.2 Material Selection.....	18
4.1.3 Manufacturing Techniques	19
4.2 Wing.....	22
4.2.1 Manufacturing Process	22
4.2.2 Material and Properties.....	22
4.3 Tail	24
4.3.1 Detailed Description	24
4.3.2 Material Selection Process.....	25
4.3.3 Manufacturing Techniques	26
5. Design Analysis	27
5.1 Final Glider Properties	27
5.2 Test Results	28
5.3 Simulations.....	29
6. Conclusion	34
7. Work Distribution	36
8. References.....	37
9. Appendix.....	38
9.1 Sample Calculations.....	38
9.1.1 Resin-Cloth Ratio Calculation.....	38

9.1.2 Composite Volume Fraction Calculation	38
9.1.3 Modulus of Elasticity Calculation	39
9.2 MATLAB Scripts.....	39
9.2.1 MATLAB PART A Glider Wing Simulation Program:.....	39
9.2.2 MATLAB PART B Glider Fuselage Simulation Program:.....	43
9.3 Engineering Drawings.....	52

List of Figures

Figure 1.1 – Parts of a Glider [2].....	1
Figure 1.2 – Aerodynamic Forces Acting on Aircraft [3]	2
Figure 2.1 – Objective Tree Diagram	3
Figure 2.2 – Given Wing Dimensions	5
Figure 3.1 – Example of Typical Glider Fuselage Design [4].....	6
Figure 3.2 – Wing Mount Configuration [7]	8
Figure 3.3 – Roll Stability [7]	8
Figure 3.4 – Conventional Tail Design [9]	9
Figure 3.5 – T-Tail Design [9].....	10
Figure 5.1 – Recorded Flight Distances of Initial Test.....	28
Figure 5.2 – M22 Airfoil Profile.....	30
Figure 5.3 – Lift Coefficient vs Angle of Attack for M22 airfoil.....	31
Figure 5.4 – Moment Coefficient vs Angle of Attack for M22 airfoil	31
Figure 5.5 – Drag Coefficient vs Angle of Attack for M22 airfoil.....	32
Figure 9.1 – Final Glider Assembly.....	52
Figure 9.2 – Exploded View of the Assembly.....	53
Figure 9.3 – Ventral Fuselage Component	54
Figure 9.4 – Dorsal Nose Shell Component	55
Figure 9.5 – Wing Platform	56
Figure 9.6 – Dorsal Foam Insert	57
Figure 9.7 – Carbon Boom.....	58
Figure 9.8 – Tail Brace	59
Figure 9.9 – Horizontal Stabilizer.....	60
Figure 9.10 – Vertical Stabilizer.....	61
Figure 9.11 – Composite Wing.....	62
Figure 9.12 – Ballast	63

List of Tables

Table 3.1– Pair-wise comparison chart.....	15
Table 3.2 – Design Concepts Morphological Chart.....	16
Table 5.1 – Bill of Materials	27
Table 7.1 - Project Work Distribution.	36

1. Introduction

The first successful heavier-than-air aircraft were unpowered gliders. The first real glider was first built during the mid-nineteenth century by British engineer George Cayley. It carried his servant on a short flight across a small valley before it crashed. [1] Over the century, gliders have become more developed and refined as newer and better technology was created. Today, gliders are commonly used for recreational purposes, as well as scientific and military applications. The main parts of a glider consist of the main wing, a fuselage, stabilizer, and the tail. These parts can vary based on materials used during manufacture as well shape. The following figure displays the basic parts of any modern glider.

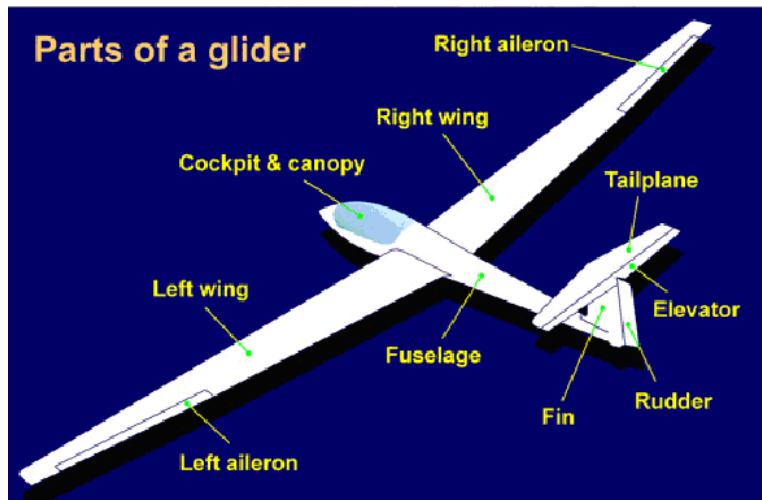


Figure 1.1 – Parts of a Glider [2]

In this project, the main purpose was to construct a glider made of a composite wing and a non-metallic fuselage. A hand-thrown glider was to be manufactured by the team members, that would move the largest possible horizontal distance when thrown. In order to do so, a long and coherent design selection process was conducted throughout. During the selection process, the aerodynamics of a glider in flight was the main priority and immensely considered for each part regarding the tail and fuselage, and the materials used to construct each.

One of the most fundamental aerodynamic measurements is lift, which is the component of force perpendicular to the oncoming flow direction of the wind. In the airplane industry, one of the most important concepts considered is the type of wing to be produced, by selecting a specific airfoil which is the cross-sectional shape of the wing. This is important because each airfoil shape has distinct characteristics which differ from one another. The four-digit NACA series is the most commonly used airfoil section worldwide. Each airfoil consequently has slightly different variations based on camber, thickness, and angle of attack, which produces lift differently. The lift coefficient is a dimensionless coefficient that relates the lift generated by a body to the density, area, and freestream velocity along the airfoil. It can be calculated with the following formula.

$$L = \frac{1}{2} \rho V_{\infty}^2 S c_L \quad (1.1)$$

Where p is the medium density, V is the freestream incoming wind velocity, C_L is the lift coefficient and S is the surface area of the wing. Drag, another aerodynamic force which opposes the motion of the incoming aircraft is also produced and acts in the same direction as the wind. Airfoils have both lift and drag coefficients. Drag can be computed using the following formula.

$$D = \frac{1}{2} \rho V_{\infty}^2 S C_D \quad (1.2)$$

Where the values are the same as equation 1.1, but with the replacement of C_L with C_D , the drag coefficient. The drag coefficient can usually be compared with the lift coefficient and can be calculated relative to one another. Since most gliders have very complex shapes, it is difficult to determine the theoretically produced drag along its airfoil. The lift-to-drag ratio is the amount of lift generated by the airfoil compared to its drag. It can be determined according to equation 1.3.

$$\frac{L}{D} = \frac{d}{h} \quad (1.3)$$

Where L is the lift, D is the drag produced, d is the horizontal distance, and h is the vertical height reached by the aircraft. Therefore, in order to develop a glider with the greatest horizontal range, a maximum value of L/D has to be reached. Figure 1.2 displays the aerodynamic free body diagram acting on the aircraft.

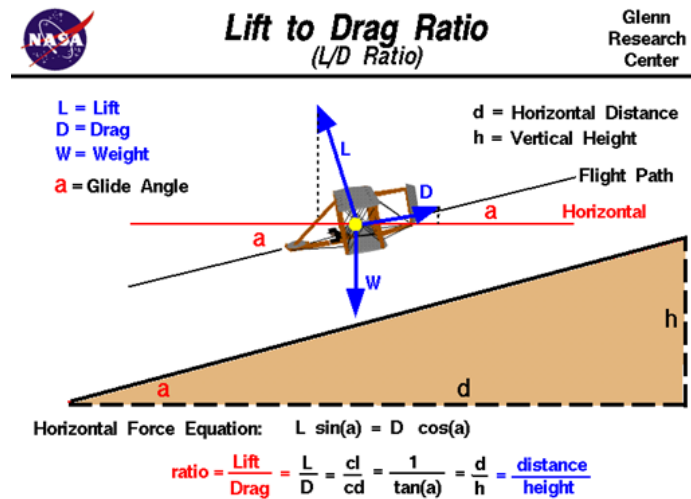


Figure 1.2 – Aerodynamic Forces Acting on Aircraft [3]

During the flight competition, the flight distance will be judged from the throwing line to the first point of contact on the floor. The overall flight score is calculated according to the following (Formula 1.4).

$$\text{Final Score} = \frac{\text{Flight Distance}}{(\text{Actual Weight} / \text{Max Weight})^2} \quad (1.4)$$

2. Problem Description

2.1 Problem Statement

Throughout the design selection process, many iterations of the fuselage and tail designs were considered until one that is both light and flies stably over a long distance is selected for the final design. The team was required to make a variety of modifications and changes with the initially design ideas to overcome various challenges and allow the functioning of the glider to be as efficient and aerodynamic as possible. The problem lies with balancing the glider due to its natural tendency to be tail heavy given that most of the mass lie being the wings. To counter act this, a counterweight must be added in from of the wing. Adding mass means that the flight score would decrease by a factor of mass squared. Over the duration, the team was able to successfully choose an ideal design through trial and error and research to create a fully functioning glider. The design process consisted of an in-depth inquiry into the challenges and hurdles presented to the team, starting from design objectives to design constraints to and design metrics.

2.2 Design Objectives

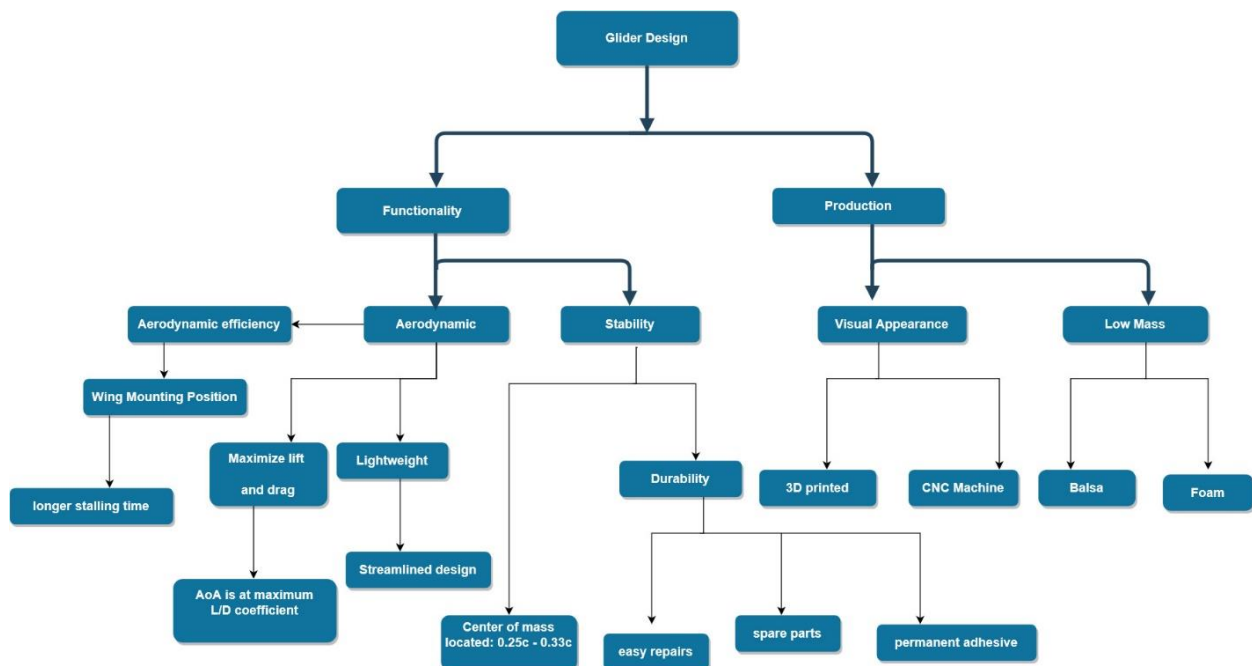


Figure 2.1 – Objective Tree Diagram

2.2.1 Design Objective List

The following list displays the overall objective list for the glider during the design selection process, explaining Figure 2.1 in more detail.

1. Glider design should be fully functional (it can fly).
 - 1.1. Design should be aerodynamic.
 - 1.1.1. Maximizes the lift and drag generated.
 - 1.1.1.1. It should result in an angle of attack with the greatest L/D ratio.
 - 1.1.2. Weight of the glider should be as minimal as possible.
 - 1.1.2.1. Design should be streamlined.
 - 1.2. Design should be aerodynamically efficient.
 - 1.2.1. Wing should be mounted at an ideal position
 - 1.2.1.1. The wing mounting position should avoid/delay stall for the longest time.
 - 1.3. Design should provide maximum stability.
 - 1.3.1. Materials should be produced durable.
 - 1.3.1.1. Allows for easy repairs and reproducibility.
 - 1.3.1.2. Allows ease of access to spare parts in case of faults.
 - 1.3.1.3. Adhesive should keep parts static and be modular for adjustments.
 - 1.3.2. Center of mass should be between quarter to a third chord from leading edge.
2. Design should be easily fabricable.
 - 2.1. Design should be appealing.
 - 2.1.1. Addition of 3D printed materials
 - 2.1.2. Addition of CNC machined materials.
 - 2.2. Reduce weight to a minimum.
 - 2.2.1. Addition of balsa wood.
 - 2.2.2. Addition of foam material.

2.3 Design Constraints

This section describes the various constraints that the project has in terms starting with the competition rules and then the one constant among all participant, the wing design.

2.3.1 Competition Rules

1. Everyone has the same wing and no control surfaces such as flaps, ailerons, elevators and rudders. Vertical winglets are permitted
2. The wings can be cut in half to induce dihedral
3. The maximum width for the fuselage is 2in (about 5.08cm)
4. Maximum horizontal stabilizer surface area is 30% of the H-Stab Surface area (about 108 in²)
5. Not metal or point parts that can cause injury
6. No wheels or rolling landing gear
7. Carbon Fiber rod tail boom. Can extend past wing leading edge, but fuse must extend past trailing edge.
8. Maximum weight limit: 200 g
9. Assembled glider must fit within 30in by 30in box
10. Judge by flight distance/weight

2.3.2 Wing Dimensions

For this competition, all participants will have the same exact wing design as seen in Figure 2.2. Note that the figure only represents an outline of how the wing should look like, there will be variations due to errors within the manufacturing phase. Also note that no two wings manufactured by each group will be identical or perfect as each wing has its own personal story to a minor flaw.

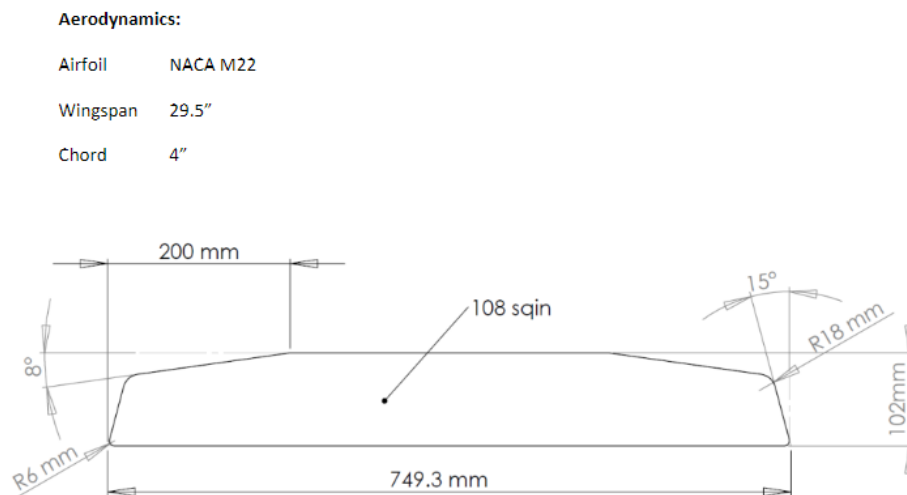


Figure 2.2 – Given Wing Dimensions

3. Design Concepts

This section will go through the process of creating a fully functional glider starting with the research of the current existing designs, then show the many stages in the development of the group's own design ideas, and finally the selection method comparing all design iterations to allow for the best one on top.

3.1 Existing Designs

This section will explain the current design for the three main parts of the glider which are the fuselage, wing, and tail. Fuselage sub section will explain the reasoning behind why high-performance glider look that way they do. Wing sub section will discuss the various ways of mounting configuration given that all participants will have the same chord, wingspan and aspect ratio. Tail sub section will explain the three common types of tail which are conventional, T-tail, and V-Tail.

3.1.1 Fuselage

Glider are incapable of producing thrust; thus, efficiency is key in order to travel long distances. Some parameters that are critical to the performance of gliders include: low profile (form) drag, low skin friction, low induced drag, low parasitic drag, low trim drag. Since the wing design has been predetermined for this project, optimization of these parameters can only be applied with regards to the design of the fuselage of the glider. As such, it was optimal to have a fuselage that had low form drag and encouraged laminar flow in order to fly longer distances. Existing designs of glider fuselages have shapes that minimize drag by optimizing said parameters. This can be seen in Figure 3.1 below.

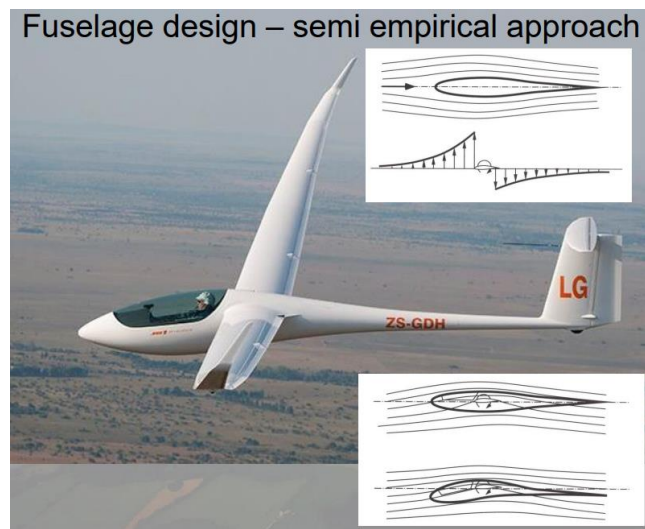


Figure 3.1 – Example of Typical Glider Fuselage Design [4]

Shape is a major factor in the selection of a design for a fuselage. A shape that minimizes the coefficient of drag is paramount for glider that intends to fly long distances. Figure 3.2 below illustrates various shapes and their corresponding coefficients of drag. It is evident that the optimal choice for a fuselage design would have to be one that incorporates the shape of an airfoil in its side profile to minimize form drag and encourage laminar flow.

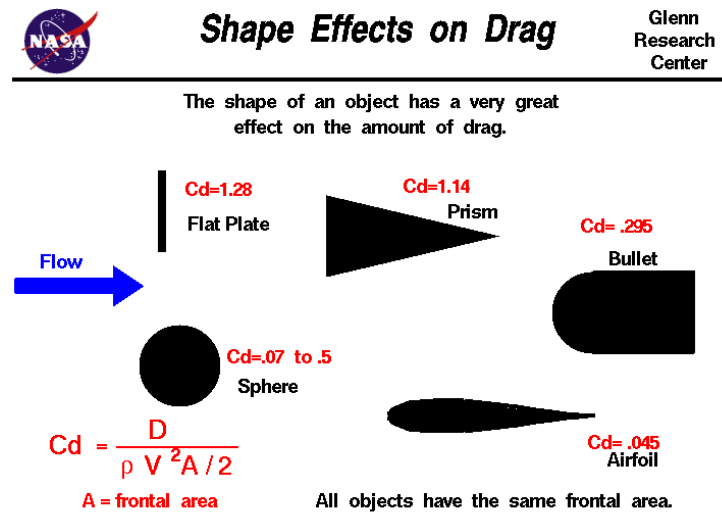


Figure 3.2 – Profile Shape Effects of Drag [5]

Another factor that can affect glider performance is the cross section of the fuselages. As seen in Figure 3.1 previously, typical glider fuselages have rounded cross-sections. It is not unusual for designers to blend shapes in attempts to minimize form drag. Some examples of Mid-sectional shapes can be seen in Figure 3.3 below.

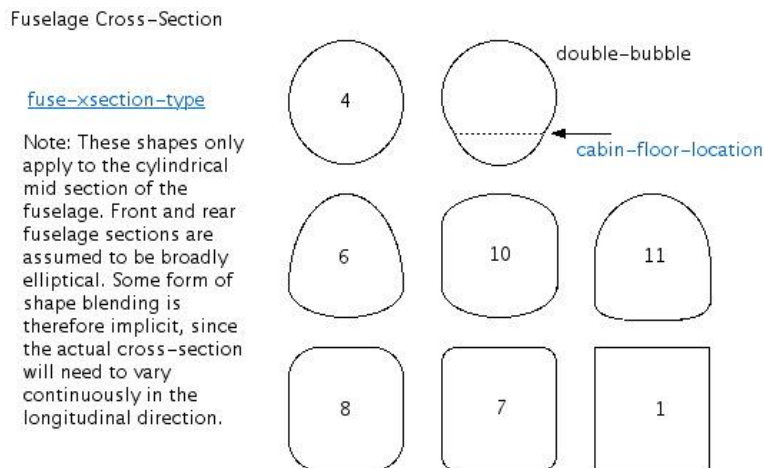


Figure 3.3 – Examples of Mid-sectional Shapes [6]

3.1.2 Wing Configurations

For this competition, one of the main constraints is that all participants will have the same exact wing design. Therefore, the only variation that will occur is with how the wings are configured in terms of how it's mounted and its angle with respect to the lateral axis.

In terms of the mounting configuration the main ones are low wing, mid wing, shoulder wing, high wing, and parasol as seen in Figure 3.2 below. By taking the two opposite mounting configuration, low and high wing, the benefits and consequences can be compared.

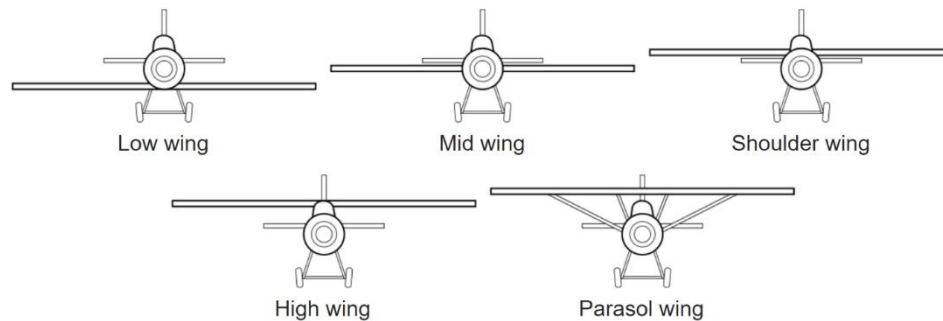


Figure 3.2 – Wing Mount Configuration [7]

By having a low wing configuration, the fuselage will be placed above the wing as well as the center of gravity. The benefits include higher roll maneuverability since it does not take a lot of aileron input to roll, which is desirable for aerobatic planes. The opposite is true for high wing plane whose center of gravity is below the wing causing the fuselage to act as a pendulum [8]. This characteristic is what makes high wing configuration to be desirable for aircraft that requires to be stable in the about the longitudinal axis with very little aileron input. This means that for this glider competition, which requires zero control surfaces, high wing would be beneficial.

Another characteristic that affects stability is dihedral and anhedral configurations, which is the angle the wing makes with respect to the pitch axis. Figure 3.3 displays the dihedral, anhedral, dihedral tips, and anhedral tips.

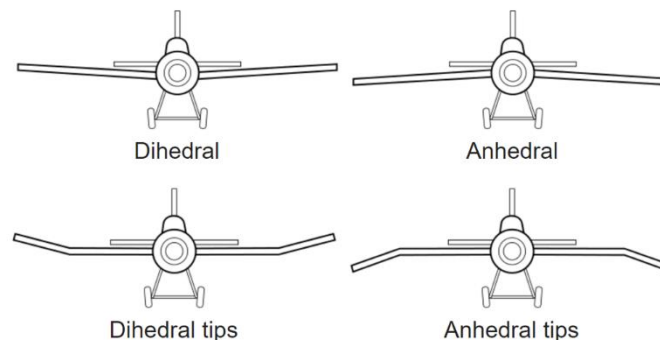


Figure 3.3 – Roll Stability [7]

Both dihedral and anhedral configurations provide stability depending on the type of aircraft. Dihedral works better with lighter planes usually with a low wing configuration. As explained

before, low wing tends to roll the plane due to the location of the center of gravity above the wing. Once the plane rolls in one direction, the imbalance of forces acting on the wing will cause it to roll in the opposite direction. Anhedral on the other hand works better for airplanes with a heavier fuselage such as the Lockheed C-5 Galaxy (a military cargo plane) Since a high wing causes the fuselage to act as a pendulum, the anhedral provides roll stability by causing it to correct itself due to the imbalance of forces acting on the wing. For this competition, the manufactured wing already has tip dihedral as part of it. Therefore, for the glider to fly straight and stable, the ideal wing configuration would be mid wing in combination with the dihedral tips.

3.1.3 Tail (T-Tail, Conventional, V-Tail)

There are many different tail configurations that each have their own benefits and drawback compared to the others. As this pertains to a glider with no control surfaces, the tail needs to be simple to manufacture. The main purpose for the tail is to counteract the pitching moment due to various aerodynamic forces. The proposed variations were the conventional tail, t-tail and v-tail designs.

Starting with the conventional tail, it is widely used in the industry as being the most “basic” form of wing. This is partly due to ease in manufacturability and little to no constraints on it. When manufacturing a conventional tail, the three stabilizers, two horizontal and one vertical can be attached to the aircraft separately, unlike some restricted designs such as the t-tail. If one chooses not to, a brace can be used instead, with a right-angle layout between the horizontal and vertical stabilizers. This tail is the most modular out of the three, as little changes to the stabilizers can be made with little to no complications. Aerodynamically, the conventional tail is effective at its job to balance the pitching moment. If the aircraft pitches up, the tail has undisturbed flow and provides moment to pitch the aircraft back down. The disadvantage to this configuration is that in steady level, the tail has the wing’s leftover air. This disturbed air makes the tail lose efficiency. The conventional tail is the most common tail design. It consists of one vertical stabilizer placed at the tapered tail section of the fuselage and another horizontal stabilizer broken into two parts, located on either side of the vertical stabilizer. For most airplanes, the conventional tail is commonly used due to its stability and control with the lowest structural weight. About three-quarters of the aircrafts in operation today including the Boeing 777 and 747, and the Airbus A300 use this tail configuration [9].

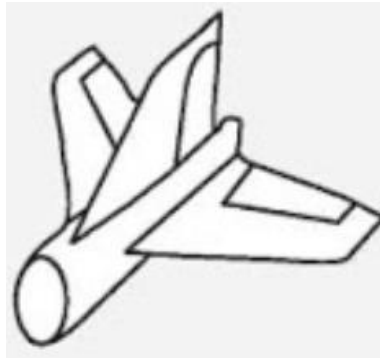


Figure 3.4 – Conventional Tail Design [9]

Ultimately, the team decided to go with the conventional tail design, since it met all requirements regarding the most stable and efficient performance of the glider. It goes to say that the conventional tail is the most commonly used tail in the aircraft industry, as it is practical, simple, and durable. Being easily manufacturable, any subsequent changes needed to be made could be done without further complications and issues. At the same time, the conventional tail has a good stability and weight.

The T-tail is a common variation of the conventional tail, with the horizontal stabilizer located at the top of the vertical stabilizer. As a result, the horizontal stabilizer ends up being above the propeller flow, and wing wake. [9] Since the horizontal stabilizer is highly efficient, the overall tail can be made smaller and lighter. The placement of the horizontal stabilizer on top of the vertical stabilizer can work to make the overall design aerodynamically efficient, and hence the size can be reduced. Some concerns regarding the T-tail, is the addition of a bending and twisting load on the vertical surface, caused by tail configuration which ultimately requires a much heavier structure than traditional designs. Also, during landing of the plane, the horizontal surfaces will produce slower and more turbulent flow of the wing wake. [9] Common airplanes that implement the T-tail design are the Boeing 727 (with its three fuselage mounted engines), and the Lockheed C-5A.

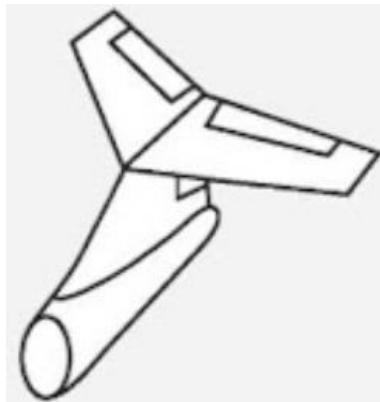


Figure 3.5 – T-Tail Design [9]

One of the key flaws about the T-tail is that it can go into a deep stall position. The theory behind this is that a tail attached to the boom will have a steady flow of air as soon as the aircraft pitches up. This allows the horizontal stabilizers to do their job and stabilize the plane back into position by cause a pitch down moment. In the T-tail, if the aircraft reaches a certain angle of attack it will stall. Not because it has reached $c_{L\text{-stall}}$, rather it goes into deep stall, which could be considered worse. Deep stall occurs when the aircraft pitches up to a point where the air going to the T-tail is the disturbed air from the wing, which restricts the tail from stabilizing the aircraft and keeping it in deep stall, see Figure 3.6 [10]. Generally, the deep stall occurs around an angle of attack from 15 to 20 degrees which is below the $c_{L\text{-stall}}$ angle in most cases [10]. This case was seen during indoor testing of the glider but seemed to not be as affected outdoors in wind. The advantage of having a clean stream of air for the tail is not worth the disadvantage of possibly going into deep stall, especially since the glider cannot have any control surfaces and electronics.

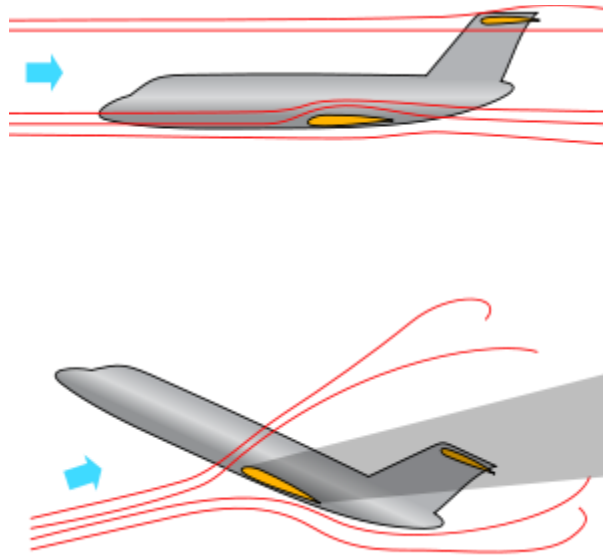


Figure 3.6 – Deep Stall Condition [10]

The V-tail design, commonly known as the ‘butterfly’ tail, was a strong candidate during the selection process for the tail configuration. It was initially selected because of its interesting design and aesthetics when arranged on the body of the glider. Unlike traditional tail designs, the V-tail consists of two surfaces that are placed neither horizontally nor vertically, but at an angle. It has had limited applications in the aircraft industry and is mainly used for transporter planes, such as Beech-craft Bonanza V-35. However, several wind studies by NASA. have shown that for the V-tail to achieve the same level of stability as a conventional tail, the V-tail area would have to be about the same size as that of a conventional tail [9].

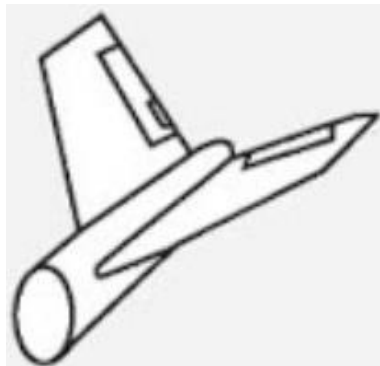


Figure 3.7 – V-Tail Design [9]

Since there are no horizontal or vertical stabilizers on the v-tail design, the challenge would be placing both angled stabilizers at equal lengths from each other, and therein lies the difficulty. At the same time, if either stabilizer were slightly misplaced at varying angles, then it would be unpredictable in its flight path during the glider competition.

3.2 Development of Designs

This section outlines the development of designs the team undertook throughout the design selection process to create the ideal glider. It displays the multi-step process both theoretically using simulations as well as experimentally through flight testing. Overall, it took three design iterations to build a functioning and efficient glider that was ultimately low in mass and had a relatively stable long-distance flight.

3.2.1 Design 1 – Initial Design Concept (Sketches)

Initial design began with the selection of the fuselage, wing and tail configurations. For the fuselage, it was selected based on the maximum allowable width as indicated in the rules and the streamline shape it had. With a fuselage length of about 25 cm, the NACA 0018 airfoil side profile fit the initial desired dimensions. The wing configuration was positioned as a mid-wing wedged by the top and bottom half of the fuselage. For the tail, the final selections were between a conventional and T-tail configuration. During this stage, a final tail design was yet to be selection and both configurations were still being considered. Initially, the T-tail provided more desirability, given that it allowed the wing and horizontal stabilizers to have a height difference. The total length of the glider was approximately 70 cm from the nose to tip, with 5 cm out of the 50 cm boom length penetrating the fuselage.

In terms of materials, the boom was 50 cm length by a 0.8 cm diameter carbon, the fuselage was 3D printed, and the tail section was 0.3175 cm thick solid balsa wood. The initial sketches regarding glider design are displayed in the following figure.

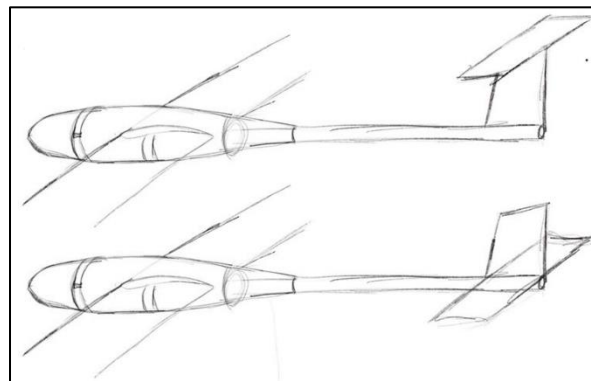


Figure 3.8 – Initial Glider Sketches

This initial design concept did not take into consideration the center of mass, center of gravity, neutral point aerodynamic center and the mass limitation. The goal during this stage of the design selection was to create a foundation for how the team envisioned the glider to look and perform during the final process.

3.2.2 Design 2 – Flight Stability (CATIA's Inertial Analysis)

Upon completion of the 3D models for the initial design, the glider was noticed to be very unbalanced. Importing all the material choices for each part, the center of gravity was located behind the wing. Theoretically, the center of mass must be in front of the neutral point for the aircraft to be stable. The goal was to position the parts so that the center of mass was located between the quarter-chord and one-third chord of the wing. Figure 3.9 displays the center of mass location for the x, y and z planes. The line spanwise is of interest since it is the axis that determines whether the design is balanced about the lateral axis.

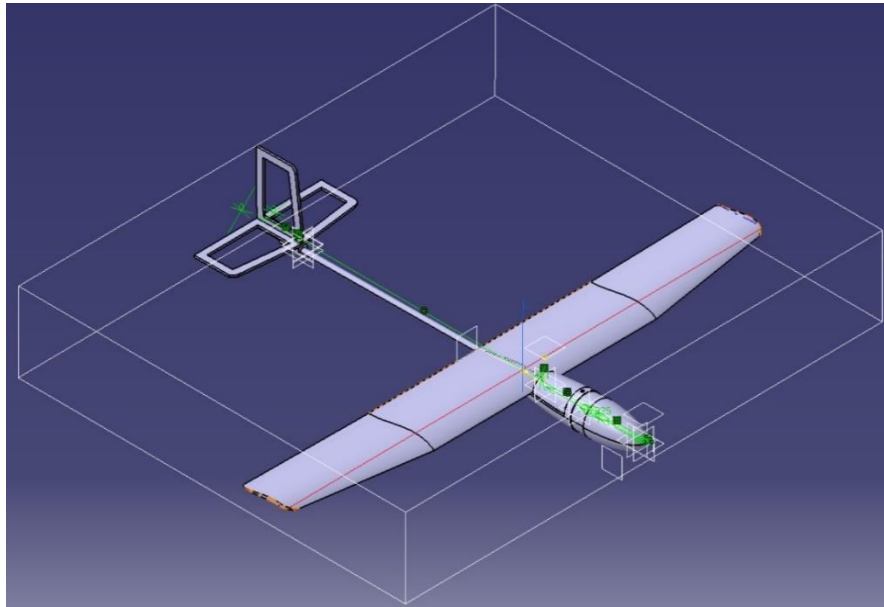


Figure 3.9 – Center of Gravity in the 3D

A few changes to the final design were incorporated at the end to adjust and allow for a much more stable, efficient, and ultimately balanced glider. The wing position was shifted further back closer to the tail, and the wing configuration was altered to a shoulder wing for easier manipulation of the wing location. At the same time, this change resulted into abandoning the initial idea of wedging the wing between the two halves of the fuselage. Instead, the top half of the fuselage was cut out in order to allow the wing to freely slide forwards and backwards.

3.2.3 Design 3 – Mass Optimization, Prototyping and Flight Tests

With the glider being balanced in all directions, the final step during the selection process was to reduce the mass of the glider as much as possible, to allow maximum flight distance as well as least weight for the highest flight score. This was achieved by changing certain materials used as well as adding lightening holes in the tail. With the mass being optimized to the maximum, the team moved onwards to the testing stage of the glider and began manufacturing.

1) The first prototype had 3D printed fuselage with a T-Tail made from balsa. The wings were attached using rubber bands and incorporated a top wing configuration. After testing, it was observed that the glider was pitching upwards too much and not able to position itself correctly at the pitching moment. Changes made after the initial flight test included replacing the T-tail with a Conventional Tail.

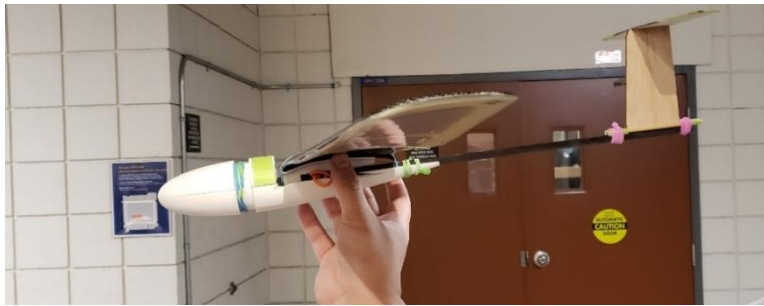


Figure 3.10 – Initial Prototype with PLA Fuselage and T-Tail Configuration



Figure 3.11 – PLA Bottom/Ventral Shell



Figure 3.12 – PLA Wing Mount

2) The second prototype consisted of the same parts used as the initial prototype, the only difference being the replacement of the T-tail with the conventional tail configuration. Using the conventional tail, the glider performed much better and was more stable during flight. It would pitch upwards not too drastically at a stable height and generate enough lift to allow the glider to go even higher. It then glided straight through the air at steady-level and landed perfectly.

3) The third prototype consisted of lighter components with a hybrid foam/3D printed fuselage. The wing was fixed securely with Velcro strips and rubber bands. Also, the tail now composed of a brace allowing it to remain aligned and attached to the boom. The tail also incorporated lightening holes for minimum weight distribution. The rest of the components and configuration were the same as the second prototype.

3.3 Design Selection

The purpose of this section was to consider and ultimately select the most efficient design concepts based on performance mentioned earlier in the report. A pair-wise comparison chart was used to compare and analyze which design concept was most suitable for optimal glider configuration. A morphological chart was also created to streamline the brainstorming process and provide a qualitative analysis of the proposed solutions. Through this evaluation, the team was able to select the most optimal design concept for the fuselage and tail.

3.3.1 Pairwise Comparison Chart

Table 3.1– Pair-wise comparison chart

Objectives	Mass	Appearance	Manufacturability	Aerodynamics	Total Score
Mass	****	1	1	0	2
Appearance	0	****	0	0	0
Manufacturability	0	1	****	0	1
Aerodynamics	1	1	1	****	3

This table contains the ranking of the various glider characteristic.

The team narrowed the characteristic of the final glider design based on its mass, appearance, manufacturability and aerodynamics. According to Table 3.1, it is evident that the aerodynamics was the most important factor when considering the designs for the tail and fuselage, with a total score of 3. Mass placed second with a score of 2, given that the flight score emphasises on reducing the glider's weight over flying a long distance. Manufacturability scores a 1 because the design can be the best theoretically, but if the team is not able to make it then we lose automatically. By knowing the tools that are available, the team can tailor the design to utilize machines such as CNC, laser cutting tool, and numerous power tools. The least important aspect of the design is the appearance with a score of 0. Although the team would like to display their talent with visual arts, it is apparent that using paint, markers and tape to add visual design can affect the aerodynamics negatively and increase the mass unintentionally. The team's priority is building a stable, fully functioning glider that will fly a long distance and with an optimized mass distribution.

3.3.2 Morphological Chart

During the design selection process, three different prototypes were tried and tested in flight. Each of one them were described in section 3.2.3.

Table 3.2 – Design Concepts Morphological Chart

Option	Wing Configuration	Components Overall Weight	Tail Selection	Flight Stability	Fuselage Material
Prototype 1	Only stable in lateral axis	High	Poor control	Low, High Pitch	Unbalanced
Prototype 2	Only unstable in longitudinal axis	Midrange	Balanced	Steady-level, High	Unbalanced
Prototype 3	Stable in all three axes	Low	Perfectly Balanced	Steady-level, High	Perfectly Balanced

This table compares the three main prototype designs developed in the design phase.

Table 3.2 represents the morphological chart that was used by the team to select the best design concept regarding the prototypes. Three different prototypes were made, and each were sufficiently tested to account for the myriad of factors affecting flight performance. The most important factors that the team took into consideration during the implementation and consideration of further changes to the gliders were: the wing configuration on the overall boom and glider, the overall weight of all the components used, the tail selection and how it affected the movement of the glider, the flight stability and pitch, and the material used for the fuselage and how it affected the balancing of parts. It is evident from that chart that the third prototype provided the best results regarding the flight testing of the glider. With the wing securely fixed in the middle with Velcro strips and rubber bands, a high lift was reached. With lightening holes in the tail, less tape used, and less materials, the overall weight of the glider was minimized. With the selection of the conventional tail, further changes were easily incorporated, and the flight was perfectly balanced without moving abruptly from top to bottom and side to side. As a result, the flight stability was top notch and remained steady level without drastic and unnecessary movement. Using a fuselage configuration of hybrid foam as well as 3D printed half-and-half, weight was reduced, and the glider was balanced perfectly from front to back.

4. Final Design Description

This section will describe the final design in terms of its geometric and aerodynamic properties. The manufacturing process as well as the material selection process are also discussed.

4.1 Fuselage

This section describes the process by which the fuselage was designed and manufactured with various materials, design techniques and airfoil data.

4.1.1 Design

The chosen side profile of the fuselage was a NACA 0018 airfoil. Although some airfoils were much more effective in encouraging laminar flow, such as the NACA 6 Series of airfoils, a symmetric airfoil allowed for ease of manufacturing and did not require any precise machining. This was done to ensure that the fuselage can be manufactured with reasonable precision and repeatability without the need of a CNC mill. Furthermore, the thickness of the airfoil was determined to be irrelevant when designing for minimal drag via XFOIL simulations. (Refer to section 5. Design Analysis). Therefore, a maximum thickness of 18% of the chord length was chosen to allow for the addition of nose ballasts if required whilst remaining within the 2-inch fuse diameter limit.

The fuselage consisted of four components. The ventral component was handcrafted and made of Styrofoam SM foam with a fuller groove at the top to accommodate space for the boom. Initially, this component was to be made using a CNC machine. However, the unavailability of the machine made it difficult to perform test flights. The front dorsal shell of the fuselage was a 1.5 mm 3D printed PLA shell reinforced with a wooden dowel. The design of the glider intended to minimize the use of 3D printed components due to the stringent mass requirements. However, it was decided that a 3D printed dorsal nose component would allow for a compartment for nose ballasts without sacrificing structural rigidity. Two pieces of balsa were placed on the flanks of the boom and fuller in order to resist the twisting and create a flat surface for the third and fourth components to rest on. The boom extended towards the rear of the PLA shell to reinforce structural integrity of the fuselage. These components can be seen in Figure 4.1 below.



Figure 4.1 – Side-profile of fuselage

The third component was a foam insert that was placed immediately to the rear of the dorsal nose shell to streamline the shape of the fuselage as well as keep the wing from yawing. The fourth component of the fuselage was the wing mount. It was a convex foam surface, matching the concave profile of the wing's underside, on which the wing can be secured in place. The wing was secured using Velcro and two rubber bands. Automotive tape was used to hold all the components of the fuselage together. Figure 4.2 shows a fully assembled fuselage with the boom attached on.



Figure 4.2 – Top view of fuselage with the boom inserted

4.1.2 Material Selection

The initial fuselage prototype made extensive use of 3D printed PLA components. However, this decision resulted in a heavy glider. The 3D printed ventral shell and wing mount weighed about 33.5 grams and 16 grams, respectively. The fully assembled glider weighed in at about 140.8 grams. Thus, it was decided that most of the 3D printed fuselage components be replaced by Styrofoam SM foam equivalents. By replacing the PLA ventral shell and wing mount with foam components, the weight was reduced to 96 grams. The PLA dorsal nose shell was retained for structural purposes albeit with its thickness reduced from 2 mm to 1.5 mm to lighten it. Overall, a 46.7% reduction in weight was achieved. This decision was a critical factor in achieving the highest score possible in the competition with the current design. Furthermore, tape was used initially to fasten the wing unto the fuselage. The tape was abandoned in favour of two rubber bands to reduce weight. This was because two rubber bands, each weighing about 0.6 grams can do the same job as 6.2 grams of tape. The Velcro, despite weighing about 2 grams, was retained to ensure the wing was firmly secured to the fuselage.

For the boom, it was initially considered that a stronger more reinforced carbon aftermarket boom would be used to ensure the structural integrity of the glider during testing. This decision stemmed from the fact that the carbon boom provided was fragile. However, the stronger boom weighed about 21.9 grams and drastically altered the balance of the glider during testing. This made it difficult to determine proper balancing for the final glider which was to make use of the lighter boom which weighed about 8.6 grams. There was a 253% weight difference between the two booms. Thus, it was decided that making use of the lighter and more fragile boom for testing was necessary for balance testing.

4.1.3 Manufacturing Techniques

At first, production of the glider's fuselage made extensive use of 3D printing. The availability of a personal 3D printer made it an attractive option given the tight schedule for manufacturing. Prior to printing, it was known that 3D printed components would be heavier than foam components. Thus, various infill settings were tested and weighed to determine the optimal ratio between durability and weight. Varying the infill settings had effects on the weight of certain 3D printed components and affected the printing time. For example, the infill was varied for the wing mount for the initial prototype. An initial print was made at 100% infill which yielded a component that weigh about 21 grams. Afterwards the infill was decreased to 50%, 25%, and 5%, weight at about 18 grams, 16 grams, and 15 grams, respectively. Printing orientation also was also an important factor in the manufacturing of 3D printed components. For the wing mount, it was determined through trial and error that vertical printing worked the best as it allowed for a more high-resolution print along the longitudinal direction. Ultimately, it was decided that 3D printing this component of the glider was too heavy as decreasing the infill beyond 5% did little to decrease the weight. Thus, this component and the PLA ventral shell of the fuselage were abandoned in favour of foam components. Furthermore, the dorsal shell was cut in half in order to reduce weight. This can be seen in Figure 4.4 below.



Figure 4.3 – 3D Printed Bottom/Dorsal Shell of Initial Prototype



Figure 4.4 – 3D Printed Components of Second Prototype

It was initially expected for the foam components to be manufactured using a CNC machine. However, the lack of availability of said machine made it difficult to produce a working prototype in time for testing. Furthermore, once obtained, the finish of the CNC component was found to be unsatisfactory, particularly the cut of the rear of the of the fuselage.

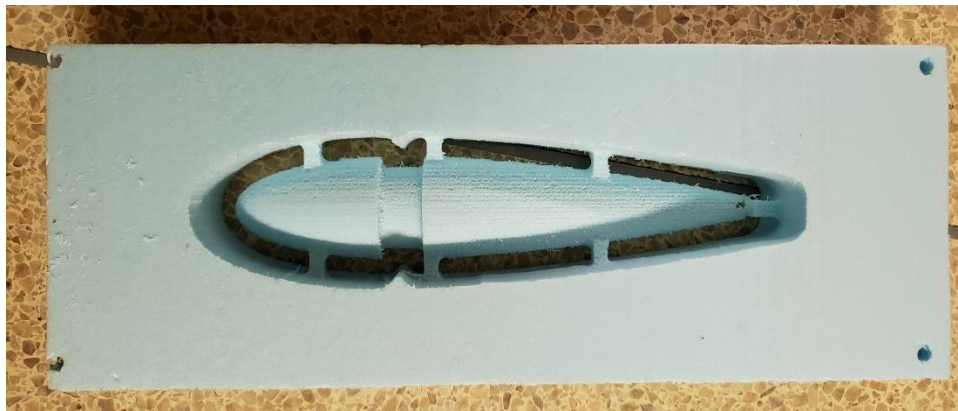


Figure 4.5 – CNC Foam Ventral Component intended for the Third Prototype

It was decided that for the third prototype, the foam replacements would be made by hand. This was done using scrap Styrofoam SM foam, a band saw, and the PLA ventral nose shell of the initial fuselage as a template. An outline of the top and side profile of the ventral component of the fuse was traced unto a piece of Styrofoam SM foam using the PLA ventral component of the initial fuse. After which a band saw was used to cut the shape of the profile and then sanded using sandpaper to shape the fuse into the desired aerodynamic shape. This resulted in a unique cross-section for the fuselage. Since the PLA dorsal component of the fuselage was retained, the assembly of said component with the new foam ventral component yielded a shape that was round at the top and square-like at the bottom with rounded edges. The shape was like #11 in Figure 3.3 above. Furthermore, the foam wing mount was made using a box cutter and sanded down to form a convex surface for the wing to rest upon. A strip of Velcro was added to secure the wing in place as was done with the PLA wing mount. A foam insert for the rear of the PLA nose shell was made by cutting a piece of foam and sanding down to an aerodynamic shape. This was done to complete the continuous airfoil profile of the fuselage. In order to create a level surface on which the mid-fuselage foam insert, and wing mount can be secured on, sheets of balsa were cut into appropriate

shapes using a boxcutter. They were placed on the flanks of the both the fuller groove and the boom on top foam ventral fuse component. Automotive tape was used to assemble all the components of the fuselage. Caution was taken when applying tape as it added unnecessary weight to the glider if overused. Thus, its use was minimized as much as possible. Overall, these modifications to the third prototype were deemed acceptable and, after numerous flight tests, were carried over to the final design.



Figure 4.6 – Handmade Foam Ventral Component used for the Third Prototype

4.2 Wing

This section goes through the process of manufacturing the composite wing as it was done as one of laboratory experiment for manufacturing techniques.

4.2.1 Manufacturing Process

The following lists the steps undertaken to manufacture the composite wing.

1. The foam frame of the wing was cut using a laser cutter and then sanded down to remove excess materials. It was weighed and its mass recorded.
2. The provided carbon and fiber glass fabrics were weighed and their mass recorded.
3. The glass fiber fabric was placed on the bottom wing mould and trimmed appropriately to fit in said mould.
4. The carbon fibre fabric was placed on the top wing mould and trimmed appropriately to fit in said mould.
5. The epoxy was mixed according to a 100:17.5 resin-to-hardener ratio. The pot life was noted to be 20 minutes.
6. With a squeegee, the epoxy mix was spread evenly along the carbon and glass fiber fabric, ensuring proper absorption. Care was taken not to damage the fiber glass fabric.
7. Fiber glass fabric was cut into appropriately shaped strips and placed along the edges of the of the bottom mould. Epoxy was applied unto these stripes.
8. Excess fiber glass fabric was cut into shorter strips for the wing ribs and placed on appropriate areas of the wing. Epoxy was applied unto these stripes.
9. The foam frame of the wing was placed on the bottom mould and the top mould was placed on top.
10. The fully assembled mould was secured using carriage bolts and heated to cure the epoxy.
11. After curing, the wing mould was disassembled, and the wing was trimmed.

4.2.2 Material and Properties

The given data from the lab questions:

	TS	E	SG (specific gravity)
MVS-410/464	9563psi	458060 psi	1.12
Carbon Fiber	318 ksi	31000 ksi	1.8
S-Glass Fiber	59 ksi	3200 ksi	2.5

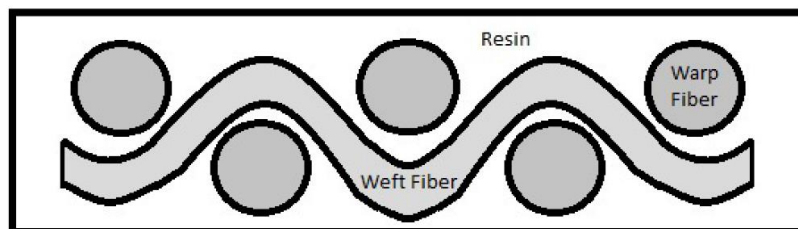


Figure 4.5 – Wing Material Properties [11]

With regards to the calculation of the mass fraction and volumetric percentage of the composite, resin-to-cloth ratio:

The initial mass of the resin was noted to be exactly 37.0 g resin and 13.2 g hardener, with 5 g of epoxy leftover. The initial mass of the carbon fiber and fiber glass was 23.3 g, with 1.5 g of fibers leftover. The non-trimmed wing had a mass of 72.7 g. The resin to cloth ratio was calculated to be 2.155, refer to Appendix 9.1.1. The fiberglass was 53% and the carbon fiber was 47% of the overall fiber mass. Note that during the layup process, extra fiberglass was given due to mistakes in layering the ribs. With the given masses, 6.861 cm^3 is carbon fiber, 4.38 cm^3 is fiberglass, and 44.821 cm^3 is epoxy, refer to Appendix 9.1.2. The total volume is 56.062 cm^3 making the carbon fiber, fiber glass and epoxy volume fractions to be 12.2%, 7.81% and 80% respectively, refer to Appendix 9.1.2.

With regards to the calculation of the modulus of elasticity of both the carbon and glass woven material:

Based on the problem, it can be assumed that the carbon fiber has a 50% weft and 50% warp, and the glass fiber has a 30% weft and a 70% warp. Also, only the material in the warp direction is used for the calculation of the tensile strength and elastic modulus. The result is carbon fiber having a modulus elasticity of 15.5 Msi and fiberglass having a modulus of elasticity of 960 ksi, refer to Appendix 9.1.3.

As was expected, the carbon fiber reinforced surface has a significantly larger modulus of elasticity than the glass fiber reinforced surface. As a result, the glass woven lower surface has a much higher stiffness value. This is an efficient result, since most airfoils tend to have a greater curve along their upper surfaces than lower surfaces, and less material stiffness would ultimately allow the wing to experience greater stress and elastic deformation before any further plastic deformation and fracturing can occur.

With regards to whether the hand layup method is superior to the RIM foam wing in terms of performance and cost:

The hand layup method is one of the most common and least expensive open-molding methods for producing a wide variety of composite products from very small to very large. It requires the least amount of equipment and the procedure essentially consists of placing fiber reinforcements by hand and then wetting with resin [12]. The reaction injection molding on the other hand, is a low pressure, low temperature procedure used to mold many types of plastic parts. Typically used for the medical, industrial, and automotive industries, RIM is often utilized for the molding of strong, lightweight parts. The process consists of two parts of polymer mixed by injecting them under high pressure into an impinging mixer and then injecting the mixture under a lower pressure into the desired mold. [13]

In terms of general performance, the reaction injection molding is superior to the hand layup method as it is done using a machine where the liquid polymers are stored in storage tanks that are dispensed by high pressure industrial pumps, versus the hand layup method which is done manually causing potential discrepancies between parts by human intervention. [13] At the same time, RIM allows it to fill molds for very large parts, offers the flexibility to design parts with significant wall thicknesses, and inserts of many types can be placed into the mold prior to RIM injection. In terms of costs, the hand layup method is the evident method. The tooling costs of the hand layup method is low, as only a mold and basic tools are required. While the RIM procedure is economical for large-volume components, the overall machine costs are significantly higher than that of the hand layup method. Overall, since the hand layup method is manual, it requires more labour and time, while the reaction injection method being mainly automated, requires less labour and time. Also, RIM is not commonly used to produce compositions like a carbon fiberglass wing, since it involves an exothermic reaction and the heat produced can potentially damage the wing. Therefore, the hand layup method is a more advantageous choice for the purposes of this project.

4.3 Tail

4.3.1 Detailed Description

The final design of the tail consists of a conventional tail setup with lightening holes to reduce the mass. The lightening holes are designed to leave a thickness of 1 cm along the stabilizer except for the H-Stab where the middle portion was 2 cm wide. This is seen through the following (Figures 9.9 & 9.10 in Appendix 9.3) Catia drafts of the horizontal and vertical stabilizers. Note that the attachment method to each other was done through a jigsaw method. The teeth of the vertical stabilizer are designed to perfectly fit into the holes of the horizontal stabilizer. The horizontal stabilizer is 20 cm wide and 7 cm long with a thickness of 0.3175 cm, refer to Figure 9.9 in Appendix 9.3. The length of it is 20 cm due to the horizontal stabilizer being one full piece instead of two separate pieces. Note that the front roots of both stabilizer pieces are filleted to induce a smooth transition.

This configuration ensures that the horizontal stabilizer, the most crucial part of the tail, does not fall out of parallel in the manufacturing process. The front sweep angle of each side is 6.34 degrees, this number comes from the two sides of the stabilizer being 1 cm shorter than middle, the longest portion. This small sweep is help channel air along the tail better, but it should be noted that in low speed applications, the effect is minimal compared to high speed ones. In turn, the sweep aided the tail in shedding some weight, as compared to a rectangular design. Note that there is no taper or sweep at the back as it is simpler to keep it rectangular and to not induce any extra uncertainties. The middle of the H-Stab has a pattern of rectangular holes spaced 0.5 cm apart from each other, each with a width of 0.3175 cm to accommodate the thickness of the V-Stab and length of 0.5 cm to match their distance apart.

The vertical stabilizer is 10 cm tall and 7 cm long with a thickness of .3175 cm, refer to Figure 9.10 in Appendix 9.3. The design of V-Stab is like that of the H-Stab, where the top of the V-Stab is 1 cm shorter than the base, resulting in a sweep angle of 6.34 degrees, the same as the horizontal. The base itself contains the jigsaw pattern to attach to the H-Stab. This pattern alternates every 0.5 cm and has a depth of 0.3175 cm that accommodates the thickness of the H-Stab.

The stabilizers attach to each other but cannot be attached to the boom directly. A brace is constructed in the shape of the following (Figure 9.8 in Appendix 9.3) Catia draft. It is 1.44 cm wide, 0.7175 cm tall and has a length of 3 cm. Every surface has a thickness of 0.3175 cm, except the bottom, which has no surface, as the boom is placed there. The top surface is intended to be flat for resting the H-Stab on. The circular holes on the two sides are meant to fit the carbon boom exactly. The long sides are meant to join the other parts together and structurally reinforce them. The draft shows the side with the boom hole, two instances of these are required in the design. The side panels are rectangles that are 2.365 cm long with a height of 0.7175 cm, two of these are required. The top surface is another rectangle that is 0.805 cm wide and 2.365 cm long.

4.3.2 Material Selection Process

The selected material for the tail and the brace that joined it to the boom is 0.3175 cm thick balsa. The material is common to come across in any hardware or wood store, with it being relatively inexpensive to buy. A sheet of 91.44 cm by 10.16 cm by 0.3175 cm was provided to each group. However, if required one member could easily get a new sheet with little to no hassle. The sheet, itself was compatible with the laser printer, making it quick and simple for a part to be made by balsa alone. This factor led the team to make and test out three different configurations of the tail in a single day. In contrast, the fuse took multiple days for each iteration, resulting in a more limited optimization time. In terms of strength and rigidity, balsa was the most optimized for its weight compared to the other available materials. On the material property list, it was the lightest wood available. Lighter materials such as depron and polystyrene were not used due to their tendency to break under load with similar dimensions. Those materials would require a significant amount of thickness to be reliable, which would increase drag to a point of inefficiency. Henceforth, balsa was the best material for the tail.

The first consideration for the brace was to use 3D printed plastic such as PLA. Due to the speed constraint of a 3D printer, the brace was optimized for balsa. There were two available sheets of balsa, and the 0.3175 cm one was chosen. Albeit, it was thicker and heavier than the .15875 cm balsa, the small design of the brace seemed negligible for weight optimization. Instead, the thicker material has a higher resistance to bending, which was extremely noticeable on the sheets themselves. Henceforth, the stronger, slightly heavier variation was used for better reliability.

4.3.3 Manufacturing Techniques

The techniques used for the tail and its braces consisted of laser printing the parts and sticking them together. The methodology for this was to create CAD drawing of the required pieces and optimize it for the laser printed material. In this case, the stabilizers were made with a jigsaw pattern to drop and lock them in place. Once the drawings were completed, the laser printer was used on the 0.3175 cm thick balsa sheet that required joining. For adhesives, CA adhesive was provided, which was strong enough to hold the pieces in place indefinitely and settles within a minute or two. For the stabilizers, the jigsaw cut-out was used as a guide, where the vertical stabilizer is required to be place perpendicular to the horizontal and pour the CA in the wedge that intersects both pieces. Ideally, to place the vertical stabilizer perfectly perpendicular required using a tool like that of a right-angle straight edge. As that was unavailable at the time, a straight edge ruler was used to estimate the placement of the v-stab. The effect of a minute offset is minor, as it would only cause yaw which is negligible in this competition. The construction of the brace is done through the same method, no jigsaw fittings. The 5 pieces for the brace are assembled in the configuration for the brace. Once held in this position, CA is carefully poured into the joint cracks and held in place until the adhesive settles. Mounting the tail onto the brace is done through CA as well. The brace is placed at the front of the tail and CA is poured into the joint cracks. Attaching the boom to the brace was planned to be done through adhesive but would be impractical if not orientated perfectly on the first try. Due to this limitation, tape was used to wrap around the boom and brace, resulting in a secure, yet modular method.

5. Design Analysis

This section will go through the analysis of the design using XFOIL, MATALAB and flight testing.

5.1 Final Glider Properties

Table 5.1 – Bill of Materials

Part No.	Part Name	Description	Qty	Theoretical Mass	Actual Mass
1	Bottom/Ventral Fuse	Bottom half of the fuselage made from SM foam	1	2.996 g	4.8 g
2	Top/Dorsal Fuse	3D printed nose piece in the top front of the fuselage made from PLA	1	12.132 g	10.7 g
3	Wing Platform	Flat surface for the wing to lie on and prevents the boom from twisting. Made from balsa	2	1.09 g	0.9 g
4	Top/Mid-Dorsal Foam Insert	Fills in the gap between the top fuse and the leading edge of the wing. Made from SM foam	1	0.893 g	1.2 g
5	Carbon Boom	Carbon fiber tube connecting the tail to the fuselage. Made from carbon	1	9.248 g	8.6 g
6	Tail Brace	Platform for the tail to lie on and aligns it along the boom.	1	0.419 g	0.6
7	Horizontal Stabilizer	Flat surface the counteract the pitching moment due to aerodynamic forces. Made from balsa	1	3.285 g	4.93 g
8	Vertical Stabilizer	Flat surface that counteracts the yaw moment keeping the glider stable about the vertical axis.	1	1.611 g	2.47 g
9	Wing	Main source of lift and drag allowing the glider to ascend and descend over a distance.	1	49.156 g	50.2 g
10	Ballast	Counterweight used to balance the plane about it aerodynamic center.	-	10 g	4.5g
11	Misc. (Tape rubber band, Velcro, etc.)	The main method of attachment is tape, while the wing used Velcro and rubber bands.	-	-	6.2g
12	Assembled Glider	Finalized Glider for Competition.		92 g	96 g

This table contains all the different parts during for the final design. Majority of the parts listed were used for the actual glider with some modification and slight changes. Theoretical mass was based off CATIA's built in inertial analysis, and actual mass were measured during the building process. Refer to appendix 9.3 for the engineering drawings all the major parts.

5.2 Test Results

With Regards to Prototype Testing:

Initial Tests;

As soon as the wing was available, testing of the glider was immediately conducted. An initial prototype was constructed using PLA components and a T-Tail configuration, as previously mentioned. Initial indoor flight tests demonstrated a tendency for the glider to pitch up. The cause was thought to be a combination of balancing issues as well as the tendency for the T-Tail to pick up disturbed airflow from the wing resulting in premature stall, aka deep stall. The average recorded flight distance of the glider was about 3.129 meters. The weight of the glider was measured to be about 119.1 grams. The average flight score of the glider was calculated to be 8.82. Significant improvements had to be made in order to achieve higher scores. Modification of the glider's mass and balancing were the top priorities.



Figure 5.1 – Recorded Flight Distances of Initial Test

Secondary Tests:

A conventional tail configuration was adopted to address the issue of pre-mature stall. This new tail increased the weight to about 126.3 grams. However, the new configuration resulted in almost three times the distance albeit with the glider tending to pitch down. Tests yielded an average distance of about 10 m. The flight score was increased to around 25.07. It was evident from these tests, that further reduction in mass as well as significant rebalancing was still required. The glider's tendency to pitch downward resulted in shorter flight distances. Furthermore, it was believed that the overall weight of the glider could still be reduced by replacing the PLA components with foam analogues. At this point, the issue concerning how well the glider is thrown plants its seed. The initial idea was to throw it whilst spinning, allowing for larger throw velocity. It was noticed that if that were to occur, the glider would have too much lift and go up to vertical and stall.

Tertiary Tests:

As previously stated, the third prototype made use of foam components as opposed to PLA. The tail weight was also reduced by introducing lightening holes in the vertical and horizontal stabilisers which were previously made of solid balsa. The holes were patched with packing tape, which weighed significantly less than the material removed. Any instances where taped was used to fasten the wing were replaced with rubber bands. Through these modifications, the weight of the glider was further reduced to about 94.8 grams at the time of testing. Flight tests with the current configuration resulted in recorded flight distances ranging from 15 meters indoors to 17.6 meters outdoors. These tests yielded scores of 66.76 to 78.33. These tests also revealed tendencies for the glider to bank to the right. It was believed that the cause of this was due to the tail tending to roll with the boom relative to the fuselage. Despite this, the third prototype was satisfactory and ready for the final design iteration. With the practise runs, the person throwing the glider was chosen, as they were the most consistent in their ability to efficiently feel the glider's potential range.

Competition Performance:

Improvements in throwing techniques resulted in better performance for the glider. This was evident during the day of the competition where the first flight achieved a record distance of about 18.6 m at a weight of about 96 grams. The added weight may have been due to the application of tape during assembly of the glider which varies with every instance of assembly. Despite the added mass, the flight score achieved was about 80.03. Once again, the glider exhibited a tendency to bank towards the right. Regardless, the performance of the glider was adequate to achieve third place in the competition.

5.3 Simulations

With regards to simulating wing performance:

To maximize range of the glider, simulations on the performance of the provided wing were conducted using XFOIL. Knowing that the wing had a mean chord length of about 0.102 m and estimating the speed of the glider to be about 10 m/s at sea level, the Reynolds number was determined to be approximately 57015. With this information, MATLAB was used in conjunction with XFOIL to simulate and plot the performance of the wing with respect to angle of attack under said conditions.

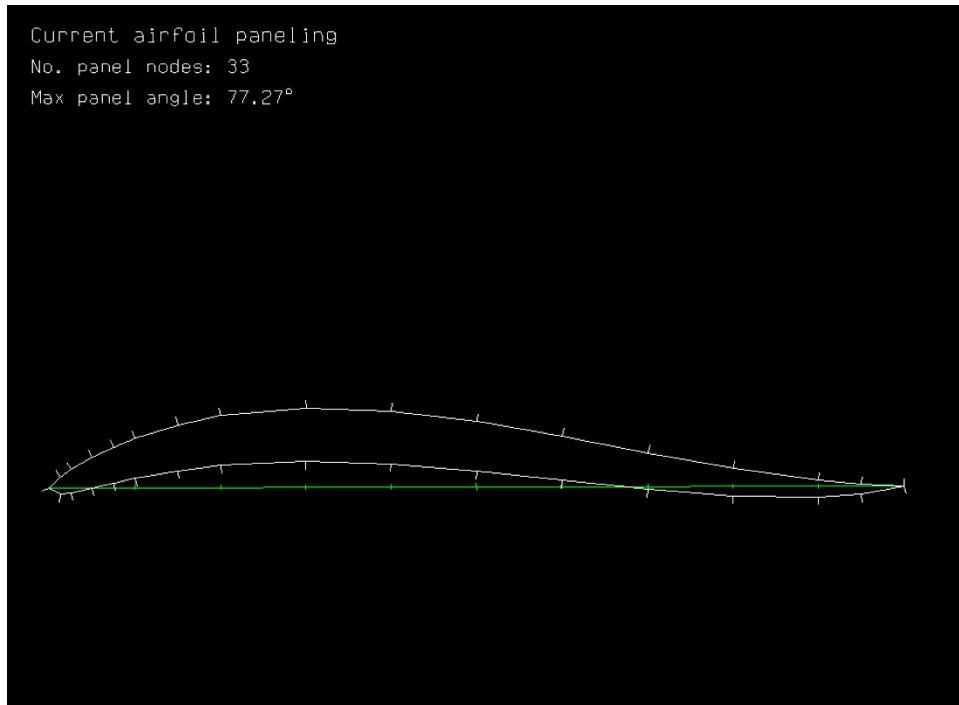


Figure 5.2 – M22 Airfoil Profile

Figure 5.2 above shows the parameters by which XFOIL simulated the performance of the M22 airfoil. The M22 airfoil coordinates was obtained from a published source:

[<https://m-selig.ae.illinois.edu/ads/coord/m22.dat>]

The coordinates were formatted appropriately and imported into XFOIL to be simulated. The simulation was set to viscous analysis at a Reynolds number of 57015 at 1000 iterations and performed sequentially from an angle of attack of -2.5 degrees to 20 degrees. The following plots were obtained via MATLAB.

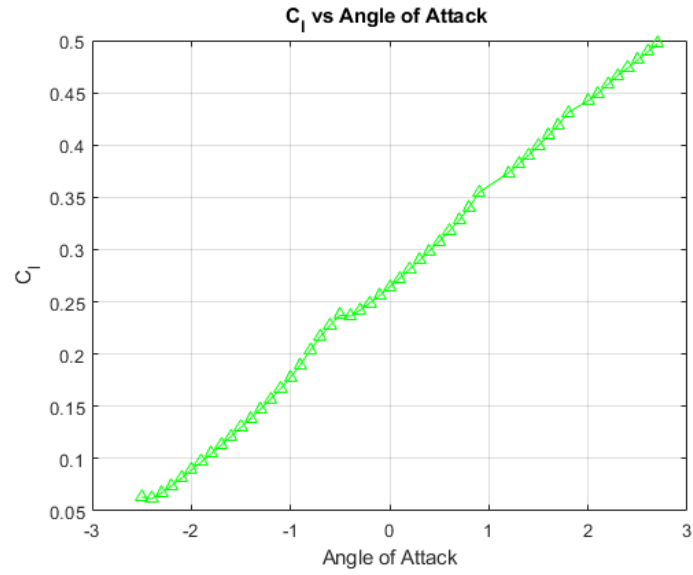


Figure 5.3 – Lift Coefficient vs Angle of Attack for M22 airfoil

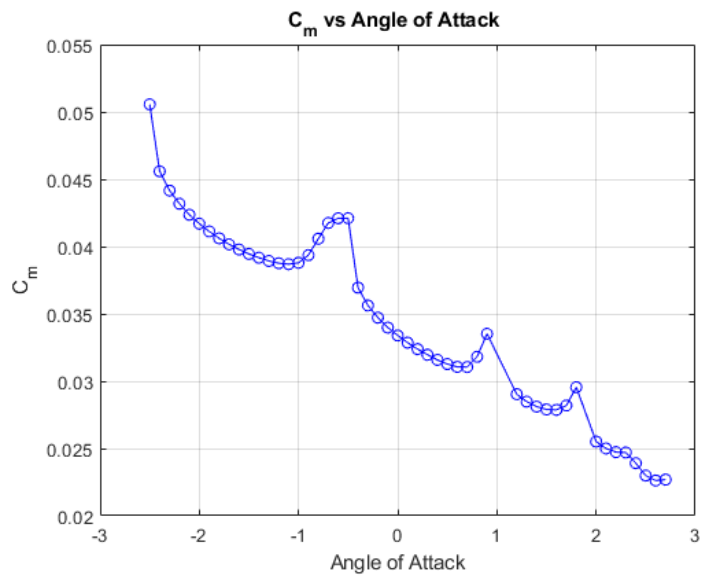


Figure 5.4 – Moment Coefficient vs Angle of Attack for M22 airfoil

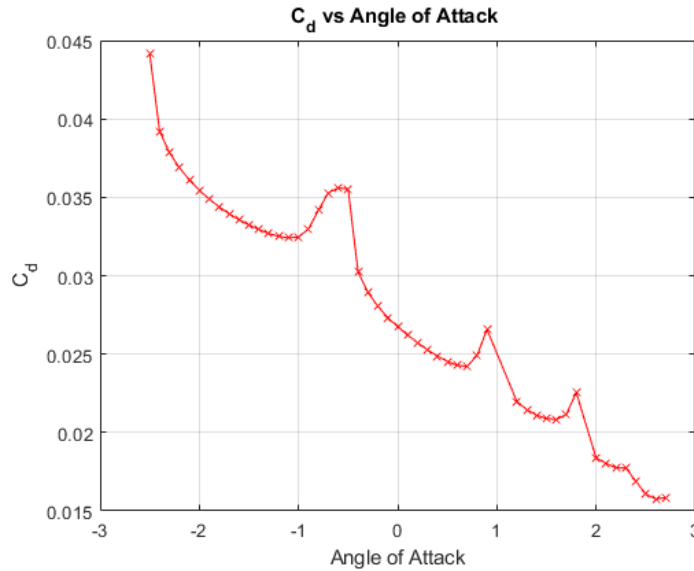


Figure 5.5 – Drag Coefficient vs Angle of Attack for M22 airfoil

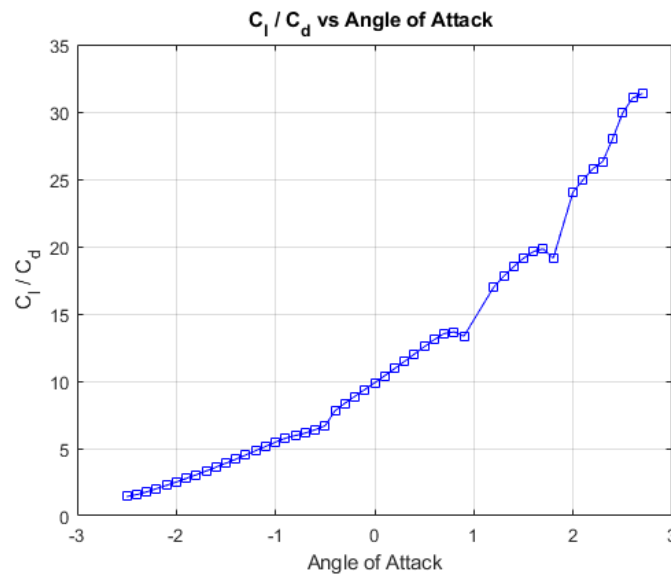


Figure 5.6 – Lift/Drag Coefficient vs Angle of Attack for M22 airfoil

The information above was to be used to analytically determine the performance of the glider and balance it accordingly. It was meant to lay out a plan on how to balance the glider and maximize lift. However, due to time constraints, it was decided that the glider be balanced via trial and error as opposed to the analytical approach. As such, the information provided by the simulation was used as a referenced on the projected performance of the glider. Furthermore, as can be seen in the data presented above, the simulation failed to converge beyond 2.5 degrees. Thus, the information might not be wholly accurate with regards to the true performance of the glider being limited only to angles of attack between -2.5 degrees and 2.5 degrees. Despite this, from the information presented by the graphs, the optimal angle of attack of the wing to produce maximum lift was at either at 2.5 degrees or beyond.

With regards to simulating and optimizing fuselage performance:

The selected shape of the glider's fuselage was decided to be an airfoil. The next step was to determine the optimal dimensions of the airfoil in order to minimize drag. Simulations were run in XFOIL to determine the effects of the maximum section thickness on the aerodynamics of the fuselage. Symmetric NACA airfoils ranging from 15% maximum section thickness to 25% maximum section thickness were simulated with angles of attack ranging from -20 to 20 degrees. At free stream velocity of 10 m/s, at sea level and a chord of about 0.254 m, the following results were found:

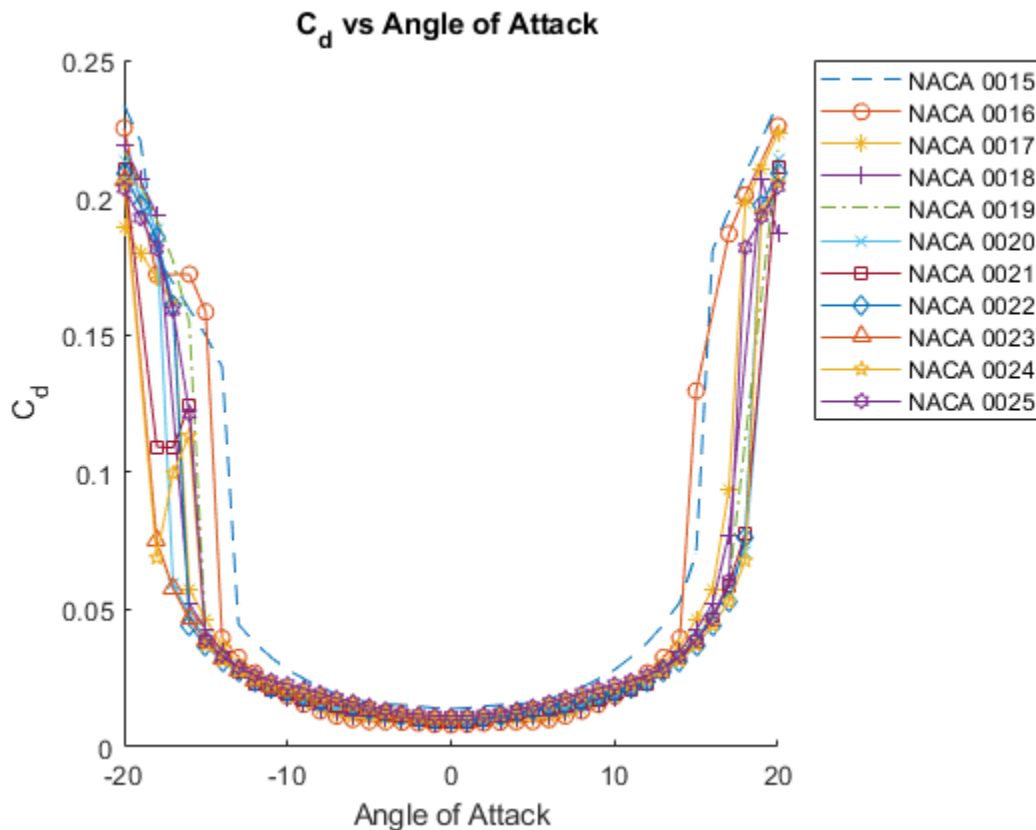


Figure 5.7 – Drag Coefficient vs Angle of Attack for various symmetric airfoils

It is evident from the data above that varying the maximum section thickness had little effect on the coefficient of drag. Despite this, the data confirms that an airfoil shape was an optimal choice for the fuselage as the coefficients of drag appear to be around 0.02 . Thus, the only limiting factor of the choice of thickness became the 2-inch diameter limit with regards to the Styrofoam SM foam material provided. For the final design, the NACA 0018 airfoil was selected which yielded a maximum section thickness of about 1.944 inches.

6. Conclusion

The project was an intuitive experience for each team. The goal was to introduce students to the various steps required in a systematic design process and impart further hands-on experience in engineering design. The team was required to build a glider within said requirements and allotted time to produce the best possible results for a glider competition. The initial brainstorming process involved multiple group meeting sessions, and initial design concepts were produced. This report documented the development of the hand thrown glider. A brief introduction of gliders and the aerodynamic concepts are given. The design process was summarized in depth, beginning with the design objectives and constraints. An objective tree and objective list were created. Next, the design concepts regarding the fuselage, wing, and tail are discussed. Existing designs were reviewed for the nose fuselage and tail, with the other parts of the glider being predetermined. The tail boom was a tubular carbon rod that extended from the nose to the fuselage to the tail. The main wing was a NACA M22 airfoil fabricated with carbon and glass fibers, as well as foam and epoxy. With the wing being already predetermined, only the way it was mounted on the glider at a specific angle could be changed. The ideal wing configuration was determined to be mid wing in combination with the dihedral tips. The conventional, T-tail, and V-tail tail designs were discussed, as well as various shapes and designs for the fuselage. The Conventional tail and an airfoil shaped structure for the fuselage were selected as the final designs. The top half of the fuselage was also cut out in order to allow the wing to freely slide forwards and backwards. The chosen side profile of the fuselage was a NACA 0018 airfoil. It was chosen due to its symmetry allowing for ease of manufacturing and not the need of a CNC mill, which was time consuming. Furthermore, the thickness of the fuselage was determined to be irrelevant when designing for minimal drag via XFOIL simulations.

Manufacturing of the entire glider and its parts began after CATIA models and drawing were created for each component. The fuselage was constructed out of Styrofoam SM foam, being extremely resilient and lightweight. The ventral shell and wing mounts were replaced with SM foam, and the nose shell was created using 3D printed PLA shells. Two pieces of balsa were placed on the flanks of the boom to allow the placement of the components. The wing was secured onto the glider using Velcro and rubber bands. Automotive tape was then used to secure all the components of the fuselage along with the boom together. Initial designs required the parts of the fuselage to be made primarily from the CNC machine. However, lack of availability and a restricted time span before testing caused it to be disregarded by the team. As a result, 3D printing of parts were extensively used, since the team had access to a personal 3D printer. Hence, both 3D printed parts and Styrofoam SM foam were both manipulated to create a balanced, lightweight fuse. The tail and brace were made using balsa wood, being easily accessible and cost-effective. Manufacturing techniques consisted of laser printing the parts and finally sticking them together. The final design of the tail consisted of lightening holes to reduce overall mass, and covered in clear tape. Using CATIA drafts, the horizontal and vertical stabilizers were attached to each other through a jigsaw method with the teeth being design to perfectly fit each other. As well, the front roots of both stabilizers were filleted to allow a smooth transition. the stabilizers were easily attached to each other and using a brace designed via CATIA consisting of circular holes on the two sides, everything was able to exactly fit the carbon boom. Further securing was done using automotive tape. Also, CA adhesive was used which was strong enough to hold the pieces in place.

A series of XFOIL simulations as well as the application of MATLAB, calculations were made to predict the lift, drag, moment, and lift-to-drag ratio coefficients of the provided wing at various angles of attack. During the development of the glider, the key goals were to create a glider with maximum lift-to-drag ratio and minimize drag, allowing the flight range to be further increased. For the wing, the Reynolds number was determined to be approximately 57015. This information was used to perform iterations at an angle of attack of -2.5 to 20 degrees. Lift, drag, and moment coefficient versus angle of attack graphs were plotted using MATLAB. The lift-to-drag ratio graph was also plotted. It was evident from the graphs that in order to create maximum lift and minimum drag, the wing would have to be mounted at approximately 2.5 to 3 degrees angle of attack to employ maximum lift. For the selection of the fuse airfoil, simulations were run on XFOIL between various symmetric airfoils to determine the effects of maximum section thickness on its aerodynamics. From the drag coefficient versus angle of attack graph plotted, it was determined that an airfoil shape was indeed the optimal design shape as the drag coefficient was about 0.2 .

Overall, this project was a valuable learning experience that provided students with a hands-on practical experience to utilize theoretical knowledge gained from the classroom experimentally in the real world. Students also gained various skills including time management, communication, and most importantly, teamwork, which are essential for real-life applications.

7. Work Distribution

Table 7.1 - Project Work Distribution.

First	Last Name	Section	%
Jann	Cristobal	6	100
Renzo	Nicolas	6	100
Pruthvi	Rajput	6	100
Awon	Sharjeel	6	100

Signature by all members:

jann C.

Renzo

Pruthvi R

Sharjeel A.

8. References

- [1] DK find out, "Early Gliders", Dorling Kindersley Limited., 2019. [Online]. Available: <https://www.dkfindout.com/us/transportation/history-aircraft/early-gliders/>
- [2] "About Gliding - British Gliding Association", British Gliding Association, 2019. [Online]. Available: <https://www.gliding.co.uk/about-gliding/#whatisgliding>. [Accessed: 29- Nov- 2019].
- [3] Nancy Hall, "Lift to Drag Ratio (L/D Ratio)", "National Aeronautics and Space Administration", May 2015. [Online]. Available: <https://www.grc.nasa.gov/WWW/K-12/airplane/ldrat.html>
- [4] H. Torode, "Efficient Light Aircraft Design - Options from Gliding", *Aerosociety*, 2019. [Online]. Available: <https://www.aerosociety.com/media/6071/4-howard-torode.pdf>. [Accessed: 28- Nov- 2019].
- [5] "Shape Effects on Drag", *Grc.nasa.gov*, 2019. [Online]. Available: <https://www.grc.nasa.gov/WWW/K-12/airplane/shaped.html>. [Accessed: 28- Nov- 2019].
- [6] "Chapter: 03. Geometric Specifications", *Lissys.demon.co.uk*, 2019. [Online]. Available: <http://www.lissys.demon.co.uk/pug/c03.html#s07>. [Accessed: 28- Nov- 2019].
- [7] "Wing configuration", *En.wikipedia.org*, 2019. [Online]. Available: https://en.wikipedia.org/wiki/Wing_configuration. [Accessed: 28- Nov- 2019].
- [8] "High Wing vs. Low Wing Aircraft (Pros, Cons, and Key Differences) | AirplaneAcademy.com", *AirplaneAcademy.com*, 2019. [Online]. Available: <https://airplaneacademy.com/high-wing-vs-low-wing-aircraft-pros-cons-and-key-differences/>. [Accessed: 28- Nov- 2019].
- [9] "Tail designs", *What-when-how.com*. [Online]. Available: <http://what-when-how.com/flight/tail-designs/>
- [10] "Deep Stall - SKYbrary Aviation Safety", *Skybrary.aero*, 2019. [Online]. Available: https://www.skybrary.aero/index.php/Deep_Stall. [Accessed: 29- Nov- 2019].
- [11] Hamid Ghaemi, Peter Bradley, "Laboratory Manual: AER507 Manufacturing and Materials", Ryerson University, Department of Aerospace Engineering, Aug. 2009. [Online]. Available: D2L
- [12] "Hand Lay-up", *Core Molding Technologies*, 2019. [Online]. Available: <http://www.coremt.com/processes/hand-lay-up/>
- [13] "What is Reaction Injection Molding", *Design Octaves*, 2019. [Online]. Available: <https://www.designoctaves.com/what-is-reaction-injection-molding>

9. Appendix

9.1 Sample Calculations

9.1.1 Resin-Cloth Ratio Calculation

$$m_{resin} = 37.0 \text{ g}; m_{hardener} = 13.2 \text{ g}; m_{epoxy} = 50.2 \text{ g}$$

$$m_{carbon \text{ fiber}} = 12.35 \text{ g}; m_{fiberglass} = 10.95 \text{ g}; m_{cloth} = 23.3 \text{ g}$$

$$m_{foam} = 14 \text{ g}$$

$$Resin: Cloth = \frac{50.2 \text{ g}}{23.3 \text{ g}} = 2.155$$

9.1.2 Composite Volume Fraction Calculation

Using the mass values from above.

$$V_{f \text{ carbon}} = \frac{m_{f \text{ carbon}}}{SG_{f \text{ carbon}}} = \frac{12.85}{1.8} = 6.861$$

$$V_{f \text{ glass}} = \frac{m_{f \text{ glass}}}{SG_{f \text{ glass}}} = \frac{10.95}{2.5} = 4.38$$

$$V_m = \frac{m_{epoxy}}{SG_{epoxy}} = \frac{50.2}{1.12} = 44.821$$

$$\sum V = V_{f \text{ carbon}} + V_{f \text{ glass}} + V_m = 6.861 + 4.38 + 44.8 = 56.062$$

$$f_{f \text{ carbon}} = \frac{V_{f \text{ carbon}}}{\sum V} = \frac{6.861}{56.062} \times 100\% = 12.2\% V$$

$$f_{f \text{ glass}} = \frac{V_{f \text{ glass}}}{\sum V} = \frac{4.32}{56.062} \times 100\% = 7.81\% V$$

$$f_m = \frac{V_m}{\sum V} = \frac{44.821}{56.062} \times 100\% = 79.99\%$$

9.1.3 Modulus of Elasticity Calculation

$$f_{carbon\ fiber\ weft} = 50\%$$

$$E_{carbon\ fiber\ weft} = f_{carbon\ fiber\ weft} \times E_{theoretical\ carbon\ fiber\ weft}$$

$$E_{carbon\ fiber\ weft} = 50\% \times 31\ 000\ ksi = 15\ 500\ ksi$$

$$f_{fiberglass\ weft} = 30\%$$

$$E_{fiberglass\ weft} = f_{fiberglass\ weft} \times E_{theoretical\ fiberglass\ weft}$$

$$E_{fiberglass\ weft} = 30\% \times 3\ 200\ ksi = 960\ ksi$$

9.2 MATLAB Scripts

9.2.1 MATLAB PART A Glider Wing Simulation Program:

Contents

- [Glider Wing Simulation](#)
- [Write and Save Commands:](#)
- [Execute XFOIL Program:](#)

Glider Wing Simulation

Code Written By: Renzo Nicolas. This Program makes use of XFOIL to calculate the aerodynamic coefficients of the wing for analysis.

```
% For a wing that has a mean chord length of 0.102 m long, at sea level and at a free  
stream velocity of 10 m/s, the Reynolds Number  
% is estimated to be: 57015
```

Write and Save Commands:

```
fid = fopen('xfoil_input.txt', 'w');  
  
% NACA M22:  
fprintf(fid, ['load m22.dat \n']); % load airfoil data  
fprintf(fid, ['OPER\n']);  
fprintf(fid, ['iter 1000 \n']);  
fprintf(fid, ['visc\n']);  
fprintf(fid, ['142116\n']);  
fprintf(fid, ['pacc\n']);  
fprintf(fid, ['naca' NACA_M22 '.txt\n']);  
fprintf(fid, ['\n']);  
fprintf(fid, ['aseq\n']);  
fprintf(fid, ['-2.5\n']);
```

```

fprintf(fid, ['20\n']);
fprintf(fid, ['0.1\n']);
fprintf(fid, ['pacc\n']);

fclose(fid);

```

Execute XFOIL Program:

```

% Execute xfoil
cmd = 'xfoil.exe < xfoil_input.txt';
[status,result] = system(cmd);

% Read Generated Data Files:

% NACA M22
fid = fopen('nacaM22.txt', 'rt');
if fid < 0
    error('error opening file %s\n', 'nacaM22.txt');
end
SM22 = textscan(fid, '%f %f %f %f %f %f %f', 'headerlines', 12);
fclose(fid);

% Plot Data:
figure('Name', 'C_l vs Angle of Attack');
plot(SM22{1}, SM22{2}, '-^', 'color', 'g');
title('C_l vs Angle of Attack ');
ylabel('C_l');
xlabel('Angle of Attack');
grid on

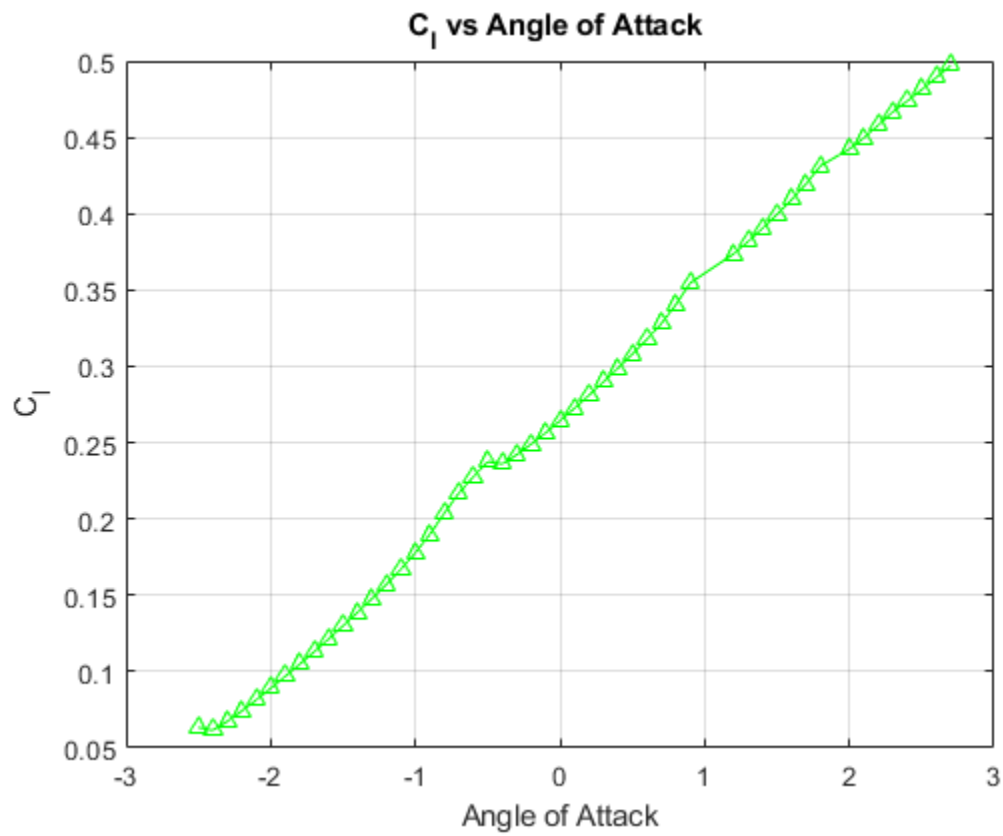
figure('Name', 'C_m vs Angle of Attack');
plot(SM22{1}, SM22{3}, '-o', 'color', 'b');
title('C_m vs Angle of Attack ');
ylabel('C_m');
xlabel('Angle of Attack');
grid on

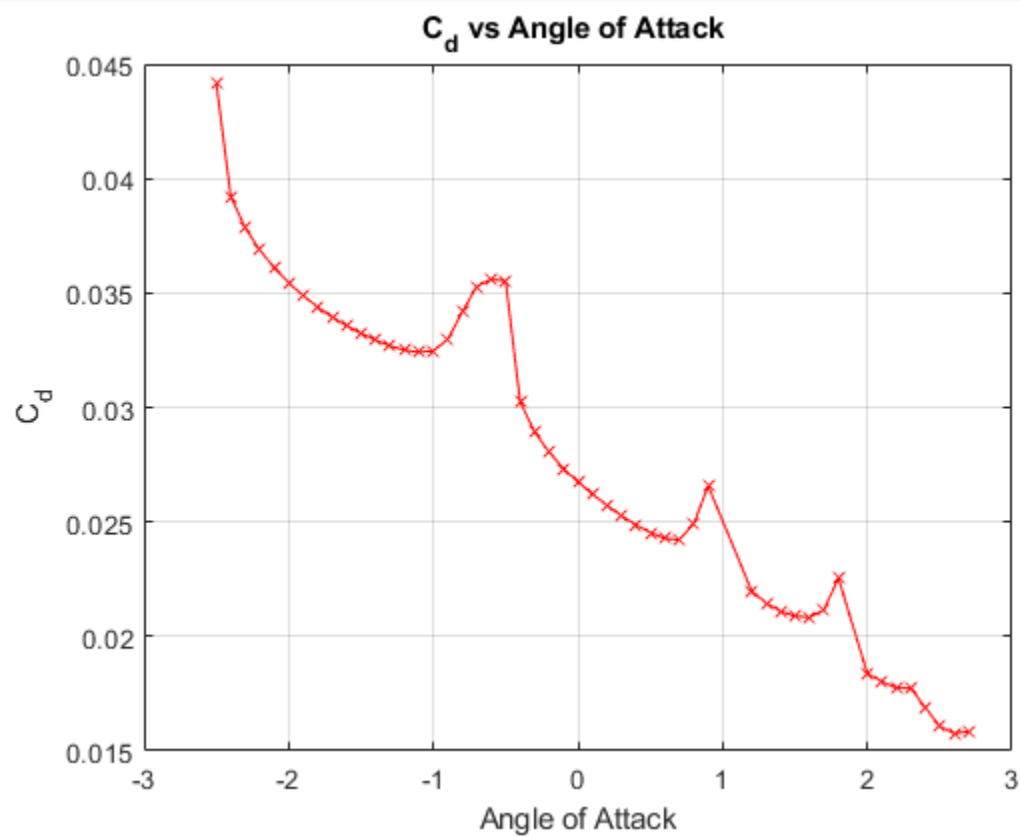
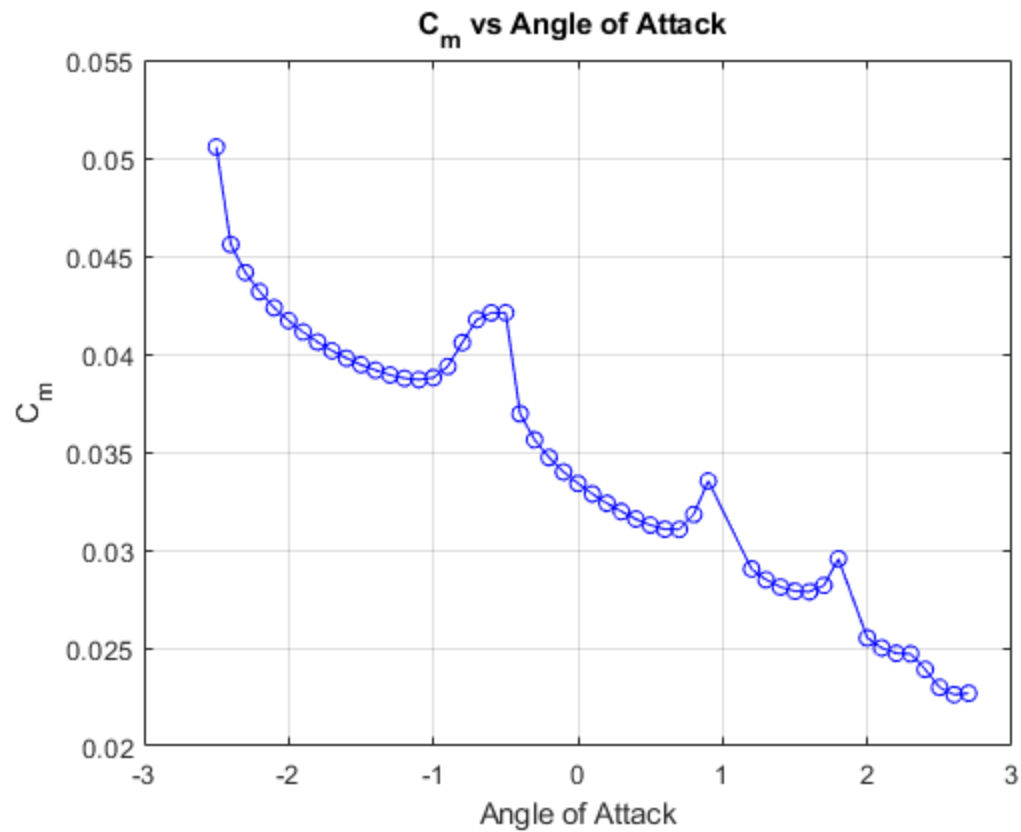
figure('Name', 'C_d vs Angle of Attack');
plot(SM22{1}, SM22{4}, '-x', 'color', 'r');
title('C_d vs Angle of Attack ');
ylabel('C_d');
xlabel('Angle of Attack');
grid on

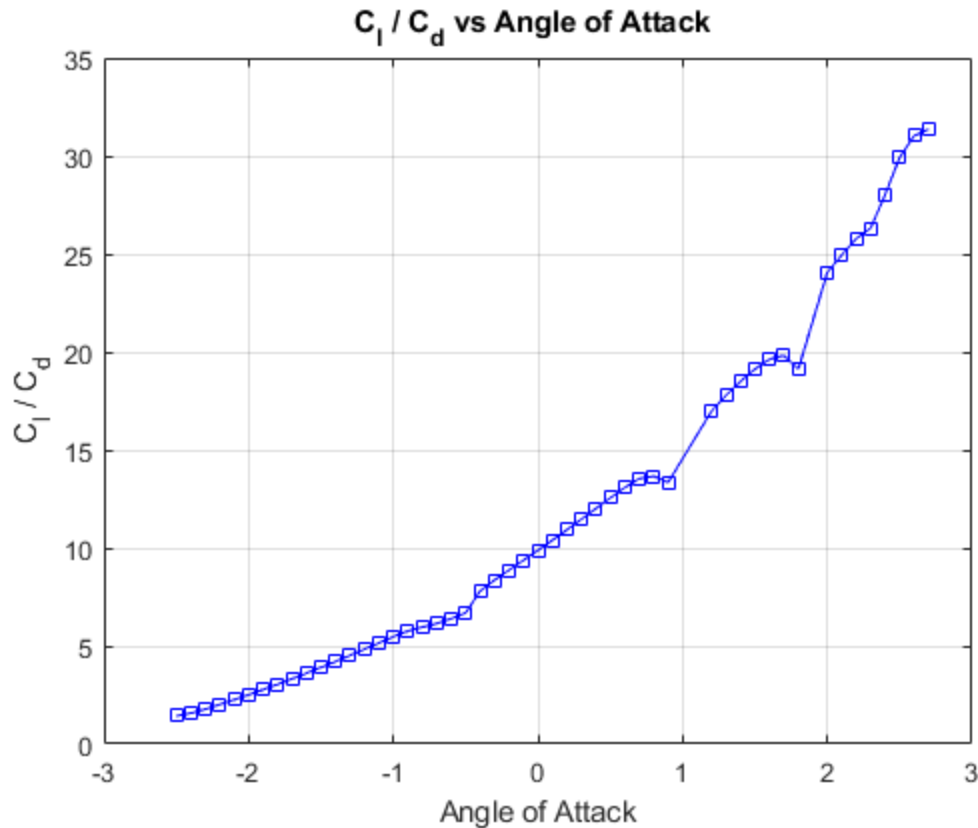
figure('Name', 'C_l / C_d vs Angle of Attack');
plot(SM22{1}, SM22{2}./SM22{4}, '-sq', 'color', 'b');

```

```
title('C_l / C_d vs Angle of Attack ');  
ylabel('C_l / C_d');  
xlabel('Angle of Attack');  
grid on  
  
% Delete Files:  
delete('NACAM22.txt');
```







Published with MATLAB® R2019a

9.2.2 MATLAB PART B Glider Fuselage Simulation Program:

Contents

- [Glider Fuselage Profile Selection](#)
- [Variable Declarations](#)
- [Write and Save Commands:](#)
- [Execute XFOIL Program:](#)

Glider Fuselage Profile Selection

Code Written By: Renzo Nicolas. This Program makes use of XFOIL to calculate coefficients of drag and plot. them against angle of attack for a selection of NACA airfoils. The best performing NACA airfoil will then be selected as the profile of the Glider Fuselage.

```
% For a fuselage that is 0.255 m long, at sea level and at a free stream velocity of
10 m/s, the Reynolds Number is estimated to be: 142116
```

Variable Declarations

```
% NACA airfoils starting from 15% Max. Thickness to 25% Max Thickness.

NACA0015 = '0015';
NACA0016 = '0016';
NACA0017 = '0017';
NACA0018 = '0018';
NACA0019 = '0019';
NACA0020 = '0020';
NACA0021 = '0021';
NACA0022 = '0022';
NACA0023 = '0023';
NACA0024 = '0024';
NACA0025 = '0025';
```

Write and Save Commands:

```
fid = fopen('xfoil_input.txt', 'w');

% NACA 0015:
fprintf(fid, ['NACA ' NACA0015 '\n']);
fprintf(fid, ['OPER\n']);
fprintf(fid, ['iter 500 \n']);
fprintf(fid, ['visc\n']);
fprintf(fid, ['142116\n']);
fprintf(fid, ['pacc\n']);
fprintf(fid, ['naca' NACA0015 '.txt\n']);
fprintf(fid, ['\n']);
fprintf(fid, ['aseq\n']);
fprintf(fid, ['-20\n']);
fprintf(fid, ['20\n']);
fprintf(fid, ['1\n']);
fprintf(fid, ['pacc\n']);
fprintf(fid, ['visc\n']);
fprintf(fid, ['\n']);

% NACA 0016
fprintf(fid, ['NACA ' NACA0016 '\n']);
fprintf(fid, ['OPER\n']);
fprintf(fid, ['iter 500 \n']);
fprintf(fid, ['visc\n']);
fprintf(fid, ['pacc\n']);
fprintf(fid, ['naca' NACA0016 '.txt\n']);
fprintf(fid, ['\n']);
fprintf(fid, ['aseq\n']);
```



```

fprintf(fid, ['-20\n']);
fprintf(fid, ['20\n']);
fprintf(fid, ['1\n']);
fprintf(fid, ['pacc\n']);
fprintf(fid, ['visc\n']);
fprintf(fid, ['\n']);

% NACA 0017
fprintf(fid, ['NACA ' NACA0017 '\n']);
fprintf(fid, ['OPER\n']);
fprintf(fid, ['iter 500 \n']);
fprintf(fid, ['visc\n']);
fprintf(fid, ['pacc\n']);
fprintf(fid, ['naca' NACA0017 '.txt\n']);
fprintf(fid, ['\n']);
fprintf(fid, ['aseq\n']);
fprintf(fid, ['-20\n']);
fprintf(fid, ['20\n']);
fprintf(fid, ['1\n']);
fprintf(fid, ['pacc\n']);
fprintf(fid, ['visc\n']);
fprintf(fid, ['\n']);

% NACA 0018
fprintf(fid, ['NACA ' NACA0018 '\n']);
fprintf(fid, ['OPER\n']);
fprintf(fid, ['iter 500 \n']);
fprintf(fid, ['visc\n']);
fprintf(fid, ['pacc\n']);
fprintf(fid, ['naca' NACA0018 '.txt\n']);
fprintf(fid, ['\n']);
fprintf(fid, ['aseq\n']);
fprintf(fid, ['-20\n']);
fprintf(fid, ['20\n']);
fprintf(fid, ['1\n']);
fprintf(fid, ['pacc\n']);
fprintf(fid, ['visc\n']);
fprintf(fid, ['\n']);

% NACA 0019
fprintf(fid, ['NACA ' NACA0019 '\n']);
fprintf(fid, ['OPER\n']);
fprintf(fid, ['iter 500 \n']);
fprintf(fid, ['visc\n']);

```

```

fprintf(fid, ['pacc\n']);
fprintf(fid, ['naca' NACA0019 '.txt\n']);
fprintf(fid, ['\n']);
fprintf(fid, ['aseq\n']);
fprintf(fid, ['-20\n']);
fprintf(fid, ['20\n']);
fprintf(fid, ['1\n']);
fprintf(fid, ['pacc\n']);
fprintf(fid, ['visc\n']);
fprintf(fid, ['\n']);

% NACA 0020
fprintf(fid, ['NACA ' NACA0020 '\n']);
fprintf(fid, ['OPER\n']);
fprintf(fid, ['iter 500 \n']);
fprintf(fid, ['visc\n']);
fprintf(fid, ['pacc\n']);
fprintf(fid, ['naca' NACA0020 '.txt\n']);
fprintf(fid, ['\n']);
fprintf(fid, ['aseq\n']);
fprintf(fid, ['-20\n']);
fprintf(fid, ['20\n']);
fprintf(fid, ['1\n']);
fprintf(fid, ['pacc\n']);
fprintf(fid, ['visc\n']);
fprintf(fid, ['\n']);

% NACA 0021
fprintf(fid, ['NACA ' NACA0021 '\n']);
fprintf(fid, ['OPER\n']);
fprintf(fid, ['iter 500 \n']);
fprintf(fid, ['visc\n']);
fprintf(fid, ['pacc\n']);
fprintf(fid, ['naca' NACA0021 '.txt\n']);
fprintf(fid, ['\n']);
fprintf(fid, ['aseq\n']);
fprintf(fid, ['-20\n']);
fprintf(fid, ['20\n']);
fprintf(fid, ['1\n']);
fprintf(fid, ['pacc\n']);
fprintf(fid, ['visc\n']);
fprintf(fid, ['\n']);

% NACA 0022
fprintf(fid, ['NACA ' NACA0022 '\n']);

```

```

fprintf(fid, ['OPER\n']);
fprintf(fid, ['iter 500 \n']);
fprintf(fid, ['visc\n']);
fprintf(fid, ['pacc\n']);
fprintf(fid, ['naca' NACA0022 '.txt\n']);
fprintf(fid, ['\n']);
fprintf(fid, ['aseq\n']);
fprintf(fid, ['-20\n']);
fprintf(fid, ['20\n']);
fprintf(fid, ['1\n']);
fprintf(fid, ['pacc\n']);
fprintf(fid, ['visc\n']);
fprintf(fid, ['\n']);

% NACA 0023
fprintf(fid, ['NACA ' NACA0023 '\n']);
fprintf(fid, ['OPER\n']);
fprintf(fid, ['iter 500 \n']);
fprintf(fid, ['visc\n']);
fprintf(fid, ['pacc\n']);
fprintf(fid, ['naca' NACA0023 '.txt\n']);
fprintf(fid, ['\n']);
fprintf(fid, ['aseq\n']);
fprintf(fid, ['0\n']);
fprintf(fid, ['-20\n']);
fprintf(fid, ['1\n']);
fprintf(fid, ['pacc\n']);
fprintf(fid, ['visc\n']);
fprintf(fid, ['\n']);

% NACA 0024
fprintf(fid, ['NACA ' NACA0024 '\n']);
fprintf(fid, ['OPER\n']);
fprintf(fid, ['iter 500 \n']);
fprintf(fid, ['visc\n']);
fprintf(fid, ['pacc\n']);
fprintf(fid, ['naca' NACA0024 '.txt\n']);
fprintf(fid, ['\n']);
fprintf(fid, ['aseq\n']);
fprintf(fid, ['-20\n']);
fprintf(fid, ['20\n']);
fprintf(fid, ['1\n']);
fprintf(fid, ['pacc\n']);
fprintf(fid, ['visc\n']);
fprintf(fid, ['\n']);

```

```

% NACA 0025
fprintf(fid, ['NACA ' NACA0025 '\n']);
fprintf(fid, ['OPER\n']);
fprintf(fid, ['iter 500 \n']);
fprintf(fid, ['visc\n']);
fprintf(fid, ['pacc\n']);
fprintf(fid, ['naca' NACA0025 '.txt\n']);
fprintf(fid, ['\n']);
fprintf(fid, ['aseq\n']);
fprintf(fid, ['-20\n']);
fprintf(fid, ['20\n']);
fprintf(fid, ['1\n']);
fprintf(fid, ['pacc\n']);
fprintf(fid, ['visc\n']);
fprintf(fid, ['\n']);

fclose(fid);

```

Execute XFOIL Program:

```

% Execute xfoil
cmd = 'xfoil.exe < xfoil_input.txt';
[status,result] = system(cmd);

% Read Generated Data Files:

% NACA 0015
fid = fopen('naca0015.txt', 'rt');
if fid < 0
    error('error opening file %s\n', 'naca0015.txt');
end
S0015 = textscan(fid, '%f %f %f %f %f %f %f', 'headerlines', 12);
fclose(fid);

% NACA 0016
fid = fopen('naca0016.txt', 'rt');
if fid < 0
    error('error opening file %s\n', 'naca0016.txt');
end
S0016 = textscan(fid, '%f %f %f %f %f %f %f', 'headerlines', 12);
fclose(fid);

% NACA 0017
fid = fopen('naca0017.txt', 'rt');
if fid < 0

```

```

        error('error opening file %s\n\n', 'naca0017.txt');
    end
    S0017 = textscan(fid, '%f %f %f %f %f %f %f', 'headerlines', 12);
    fclose(fid);

    % NACA 0018
    fid = fopen('naca0018.txt', 'rt');
    if fid < 0
        error('error opening file %s\n\n', 'naca0018.txt');
    end
    S0018 = textscan(fid, '%f %f %f %f %f %f %f', 'headerlines', 12);
    fclose(fid);

    % NACA 0019
    fid = fopen('naca0019.txt', 'rt');
    if fid < 0
        error('error opening file %s\n\n', 'naca0019.txt');
    end
    S0019 = textscan(fid, '%f %f %f %f %f %f %f', 'headerlines', 12);
    fclose(fid);

    % NACA 0020
    fid = fopen('naca0020.txt', 'rt');
    if fid < 0
        error('error opening file %s\n\n', 'naca0020.txt');
    end
    S0020 = textscan(fid, '%f %f %f %f %f %f %f', 'headerlines', 12);
    fclose(fid);

    % NACA 0021
    fid = fopen('naca0021.txt', 'rt');
    if fid < 0
        error('error opening file %s\n\n', 'naca0021.txt');
    end
    S0021 = textscan(fid, '%f %f %f %f %f %f %f', 'headerlines', 12);
    fclose(fid);

    % NACA 0022
    fid = fopen('naca0022.txt', 'rt');
    if fid < 0
        error('error opening file %s\n\n', 'naca0022.txt');
    end
    S0022 = textscan(fid, '%f %f %f %f %f %f %f', 'headerlines', 12);
    fclose(fid);

```

```

% NACA 0023
fid = fopen('naca0023.txt', 'rt');
if fid < 0
    error('error opening file %s\n\n', 'naca0023.txt');
end
S0023 = textscan(fid, '%f %f %f %f %f %f %f', 'headerlines', 12);
fclose(fid);

% NACA 0024
fid = fopen('naca0024.txt', 'rt');
if fid < 0
    error('error opening file %s\n\n', 'naca0024.txt');
end
S0024 = textscan(fid, '%f %f %f %f %f %f %f', 'headerlines', 12);
fclose(fid);

% NACA 0025
fid = fopen('naca0025.txt', 'rt');
if fid < 0
    error('error opening file %s\n\n', 'naca0025.txt');
end
S0025 = textscan(fid, '%f %f %f %f %f %f %f', 'headerlines', 12);
fclose(fid);

% Plot Data:
figure('Name', 'Thickness Comparison');
hold on
plot(S0015{1}, S0015{3}, '--');
title('C_d vs Angle of Attack ');
ylabel('C_d');
xlabel('Angle of Attack');

plot(S0016{1}, S0016{4}, '-o');
plot(S0017{1}, S0017{4}, '-*');
plot(S0018{1}, S0018{4}, '-+');
plot(S0019{1}, S0019{4}, '-.');
plot(S0020{1}, S0020{4}, '-x');
plot(S0021{1}, S0021{4}, '-s');
plot(S0022{1}, S0022{4}, '-d');
plot(S0023{1}, S0023{4}, '-^');
plot(S0024{1}, S0024{4}, '-p');
plot(S0025{1}, S0025{4}, '-h');

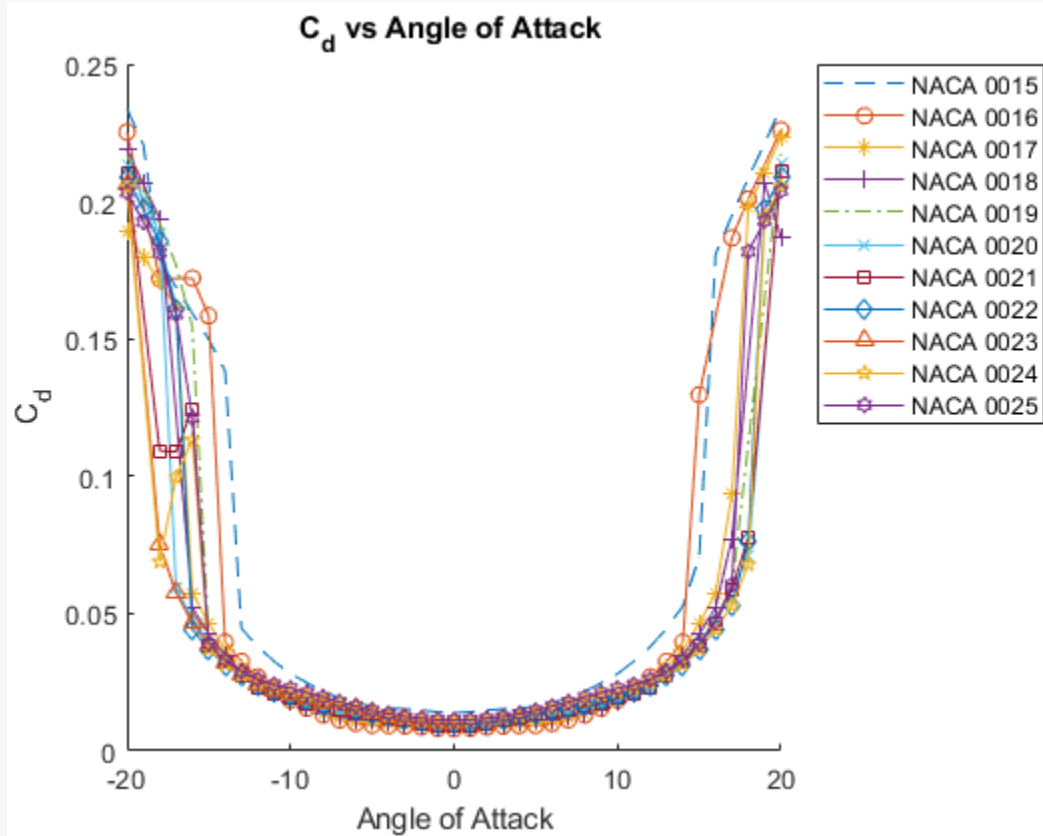
```

```

legend({'NACA 0015', 'NACA 0016', 'NACA 0017', 'NACA 0018', 'NACA 0019', 'NACA 0020', 'NACA 0021', 'NACA 0022', 'NACA 0023', 'NACA 0024', 'NACA 0025'}, 'Location', 'bestoutside');
hold off

% Delete Files:
delete('naca0015.txt');
delete('naca0016.txt');
delete('naca0017.txt');
delete('naca0018.txt');
delete('naca0019.txt');
delete('naca0020.txt');
delete('naca0021.txt');
delete('naca0022.txt');
delete('naca0023.txt');
delete('naca0024.txt');
delete('naca0025.txt');

```



9.3 Engineering Drawings

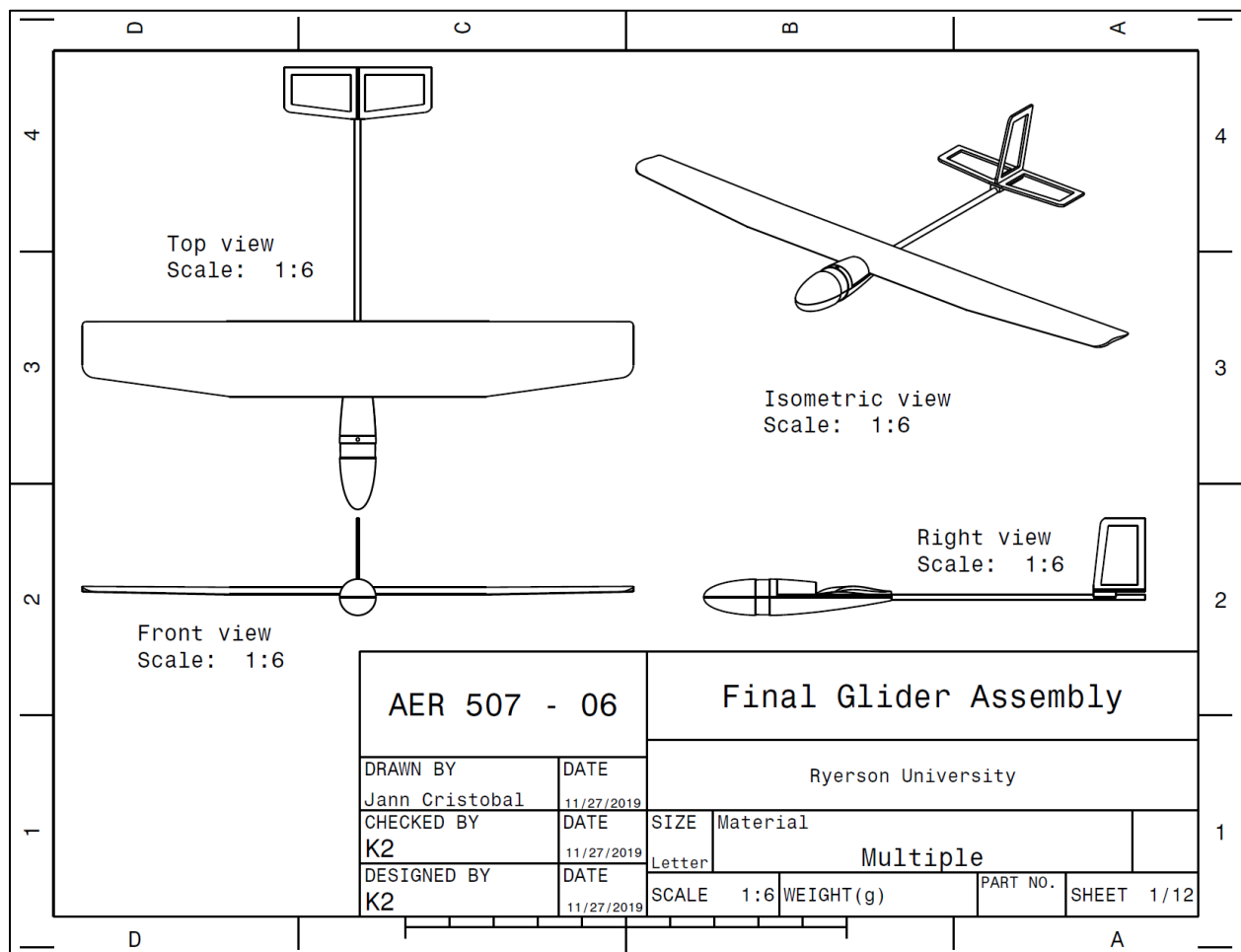


Figure 9.1 – Final Glider Assembly

This is the intended final product once all the parts are manufactured and assembled. The main method of attachment are Velcro, tape, and rubber bands which are not shown in the drawings.

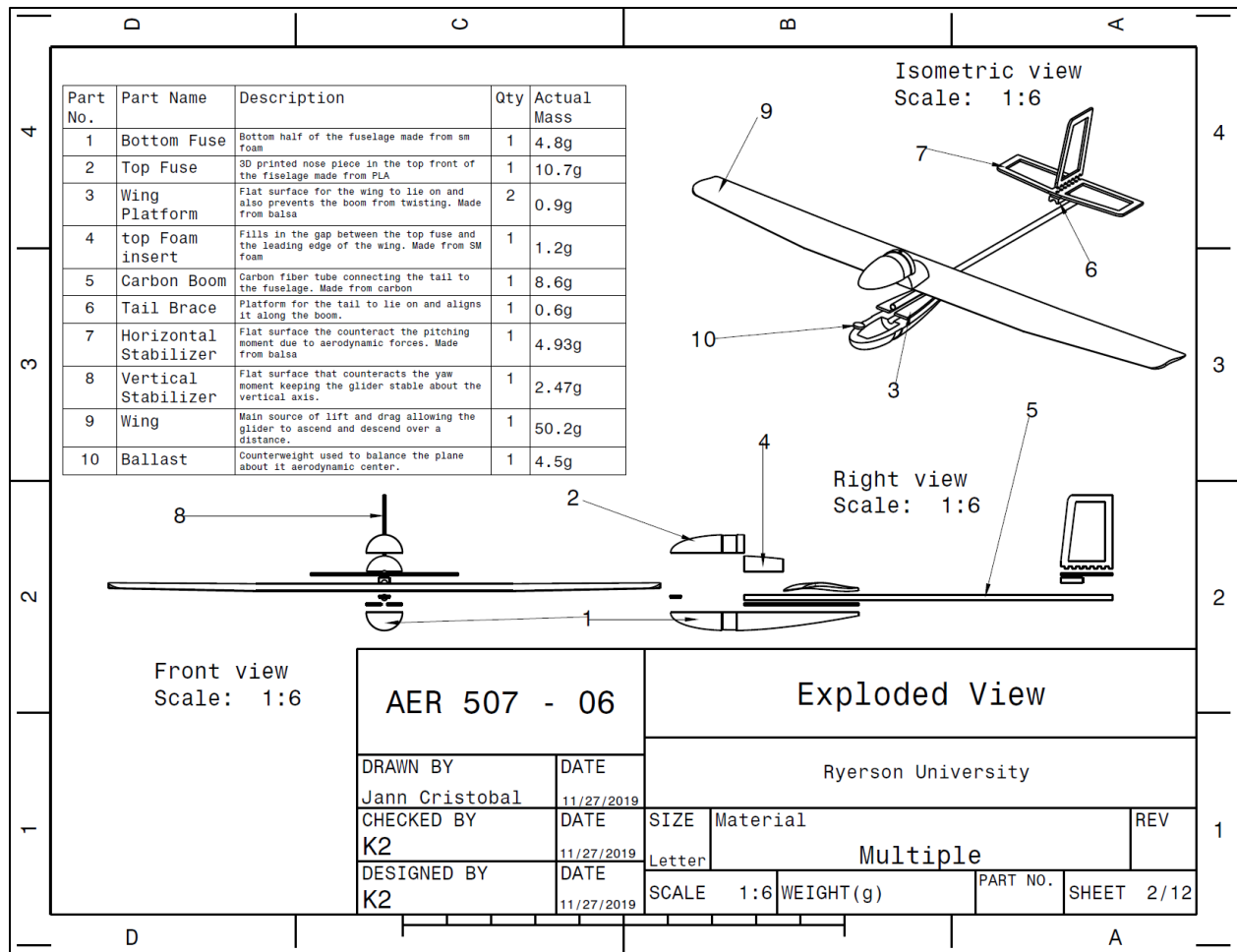


Figure 9.2 – Exploded View of the Assembly

This is an exploded view of the assembly showcasing the parts that were hidden in the final glider assembly. The list of bill of materials is also here as well as the labels for all the different parts of the glider.

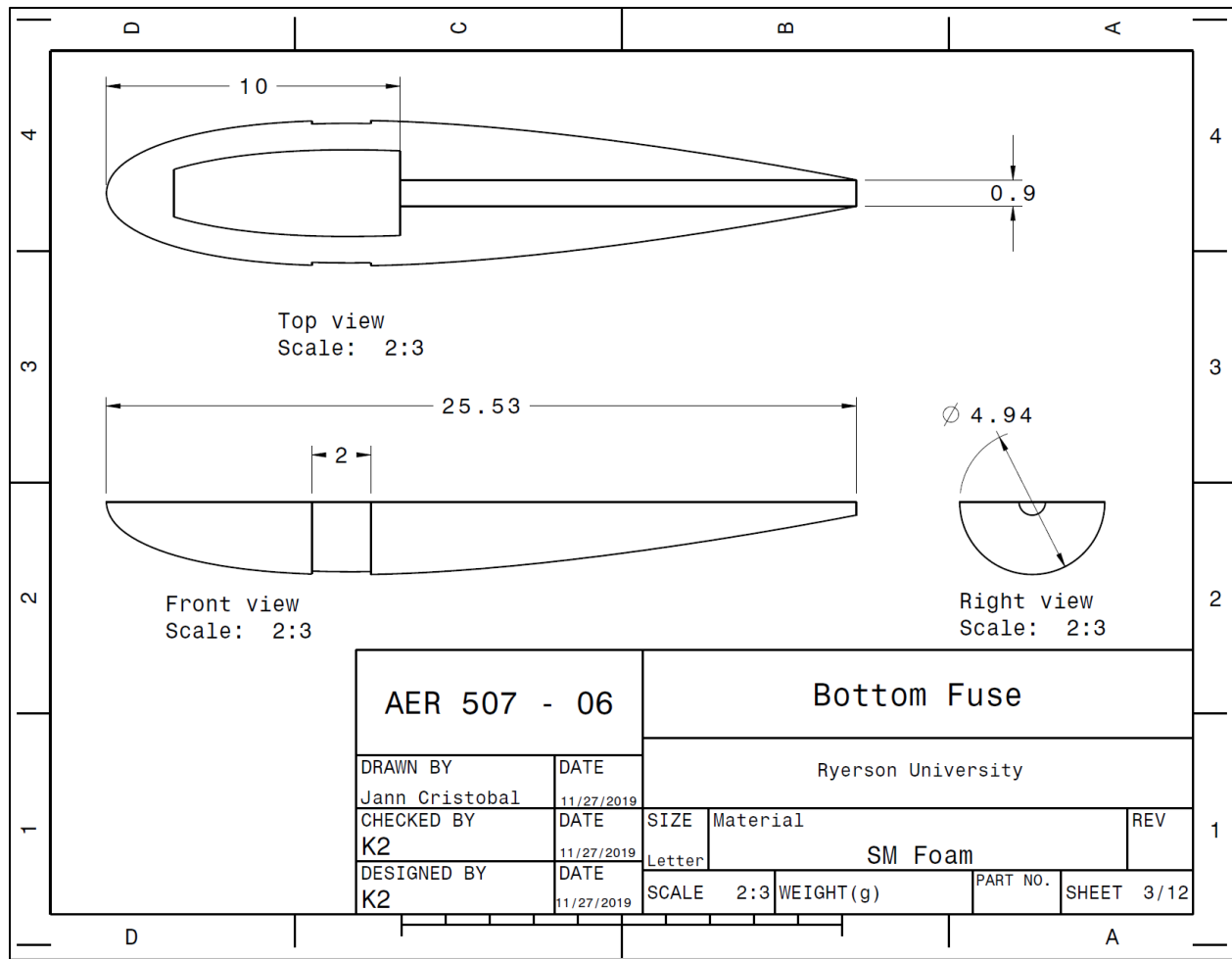


Figure 9.3 – Ventral Fuselage Component

This is the bottom half of the fuselage which is made from SM foam. The intricate design shape requires the use of CNC milling machine. Another option for manufacturing is to use bandsaw and sandpaper to get the desired shape.

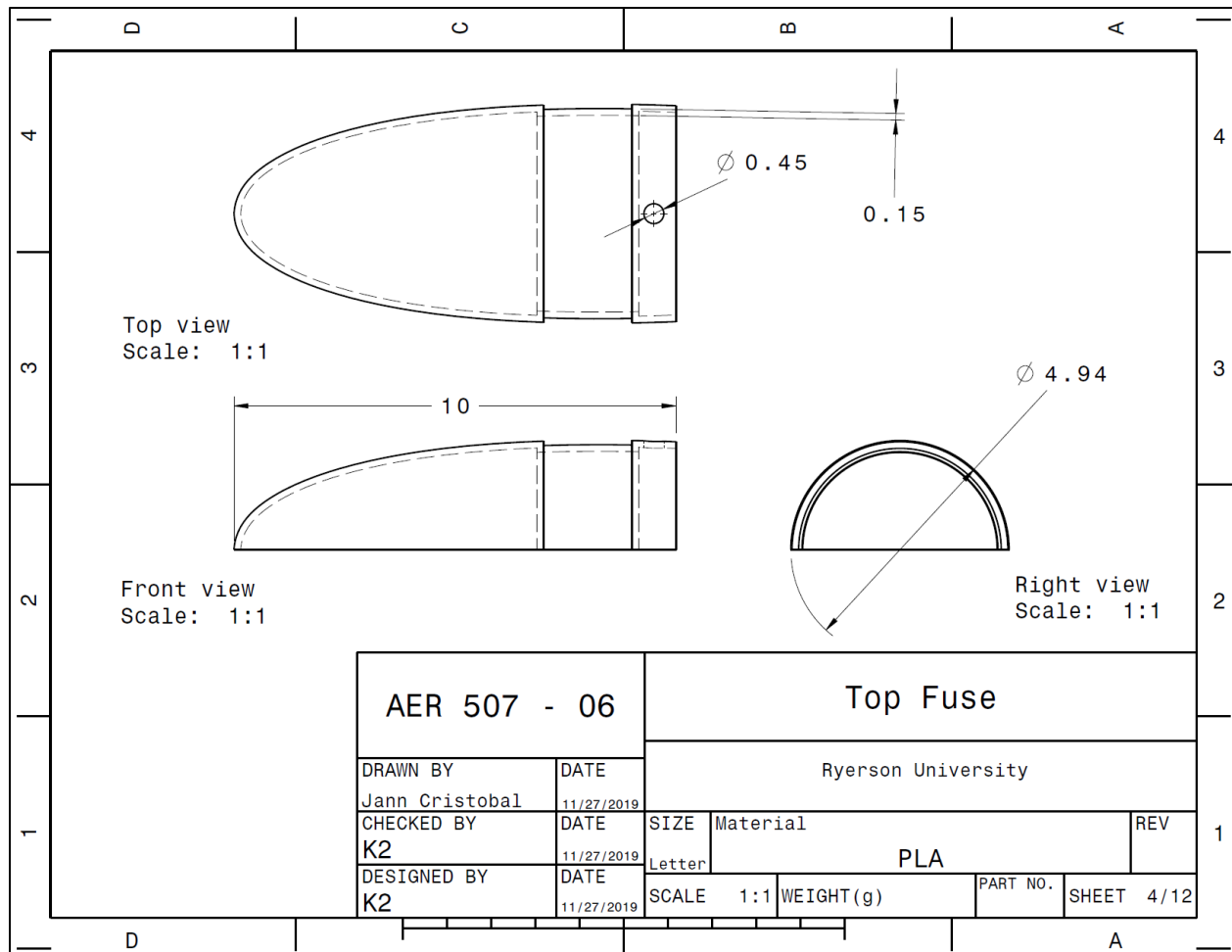


Figure 9.4 – Dorsal Nose Shell Component

This is a hollowed part meant shell the from part of the fuse where counterweights will be placed. The groove is mean for the tape that will be used to attach it with the bottom fuse. It is 3D printed using PLA.

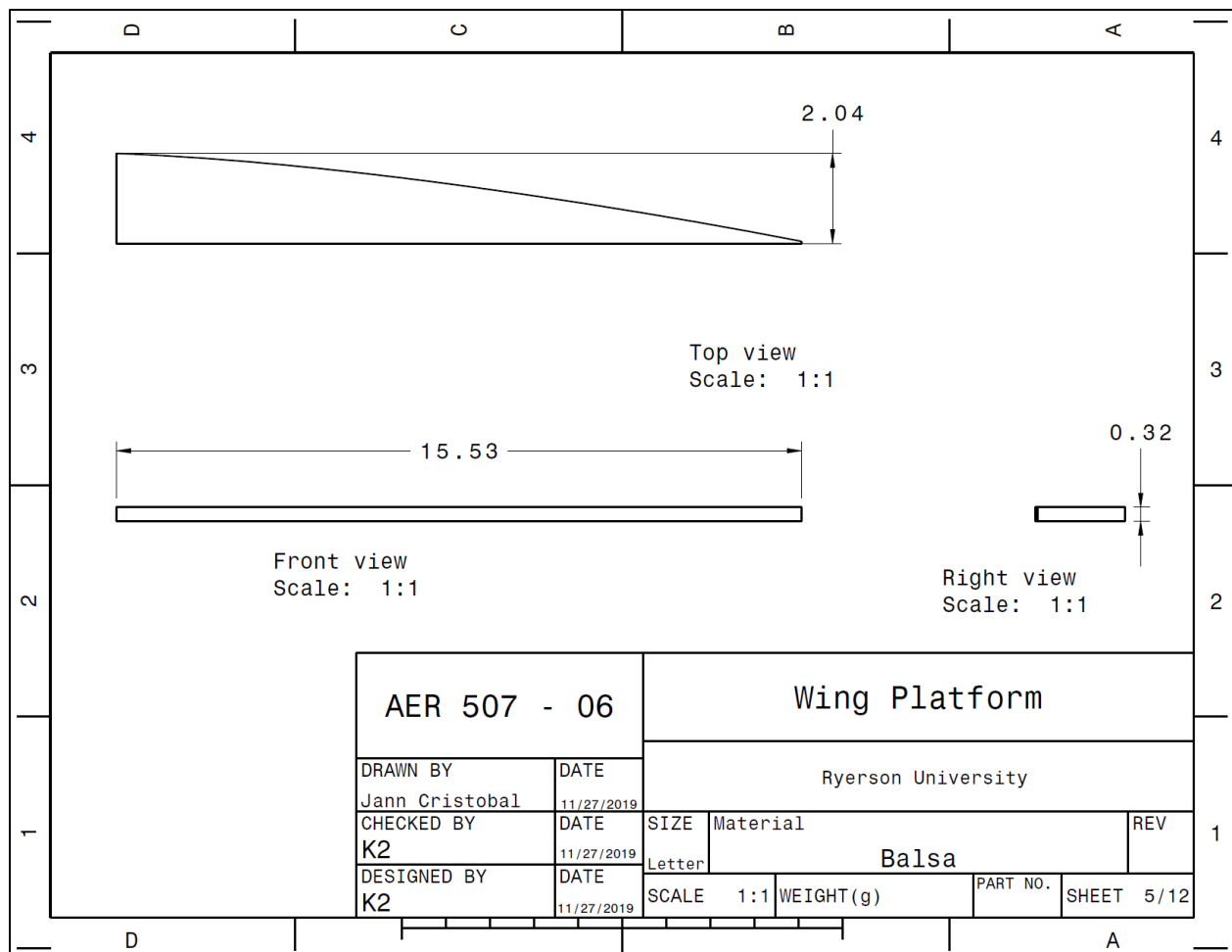


Figure 9.5 – Wing Platform

This is a platform laser cut from balsa wood. The main purpose is for the wing to have a flat surface to align with without damaging the foam. Secondary purpose is to help eliminate the twisting of the boom.

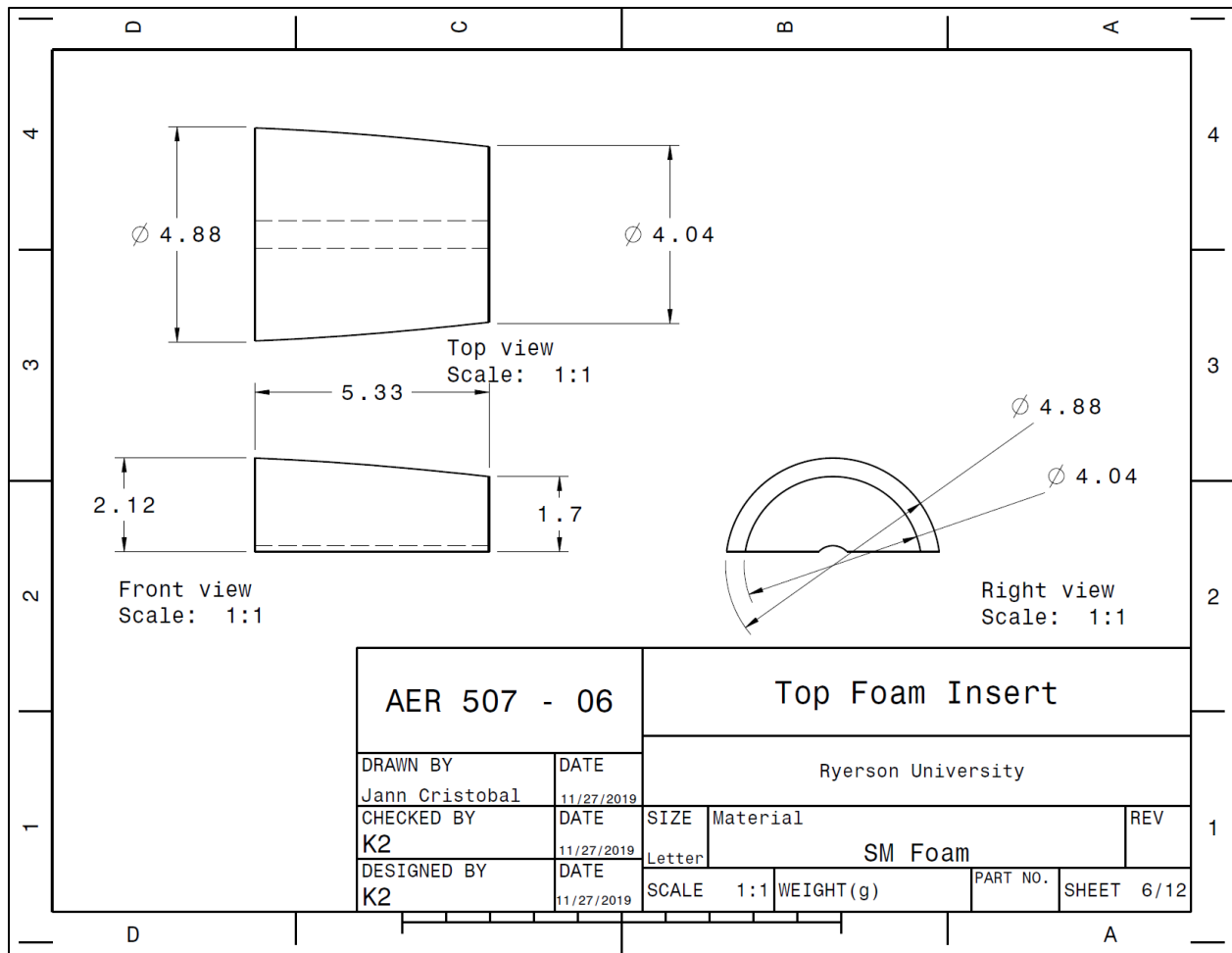


Figure 9.6 – Dorsal Foam Insert

This part is meant to fill in the gap between the top fuse and the wing to allow for a more streamline design without adding too much weight. This insert helps with keeping the wing from any unwanted movement about the three axis of rotation.

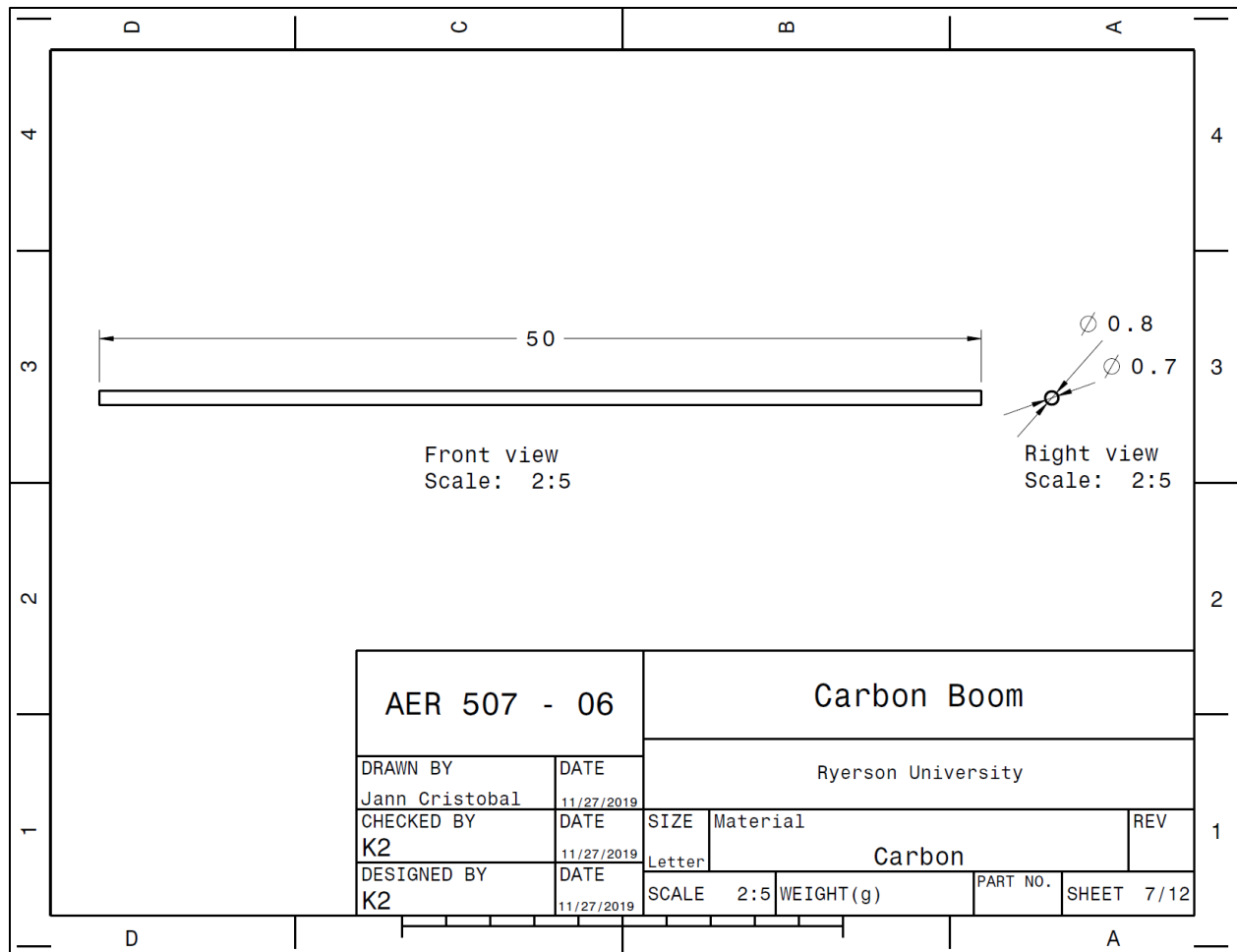


Figure 9.7 – Carbon Boom

This is the provided carbon fiber boom. It is the lightest material for its purpose but in terms of long-term strength it is lacking. The ends break easily with minimal force, but is good enough for the flight test and competition.

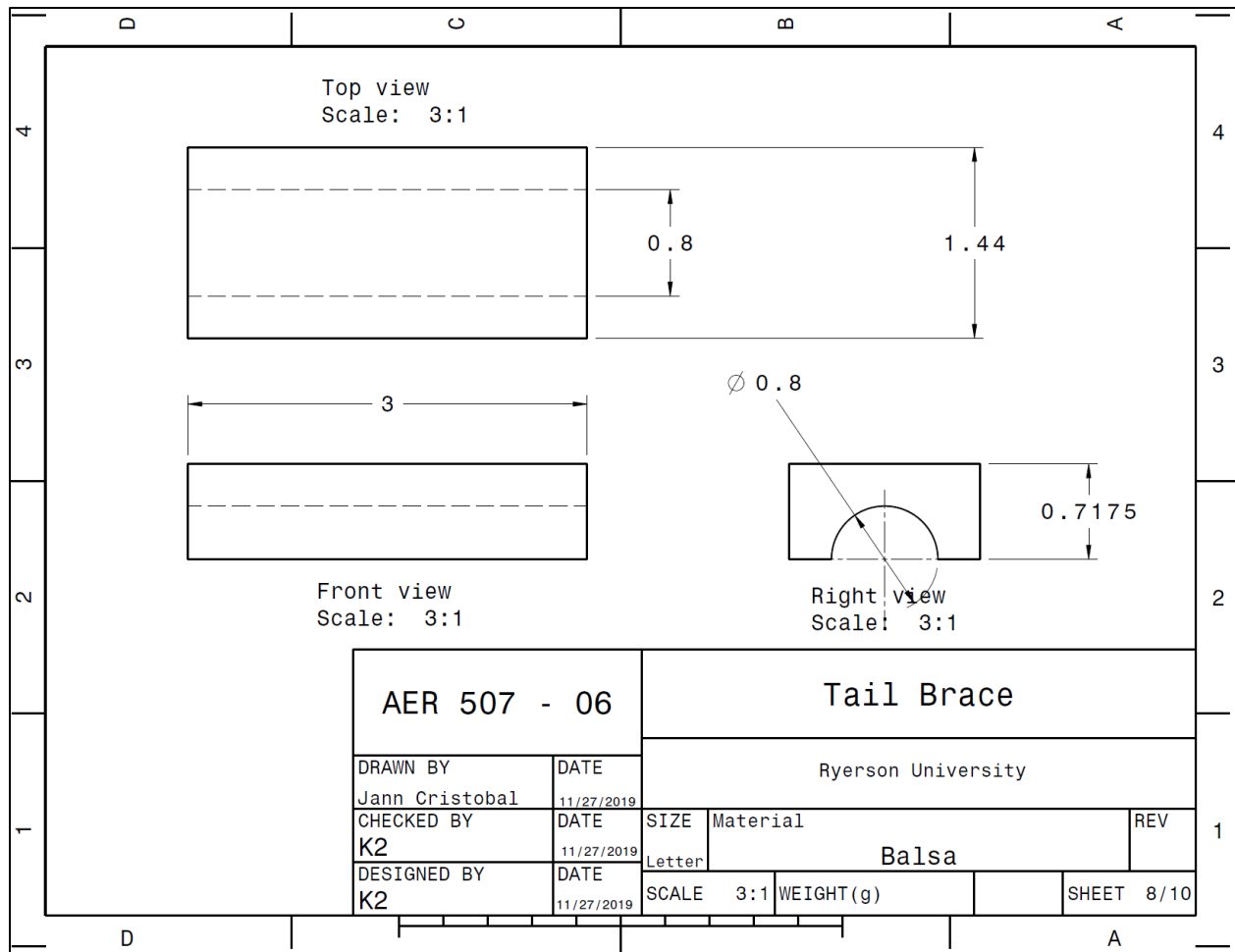


Figure 9.8 – Tail Brace

This is the brace that will act as the flat surface for the tail to attach on and keep them aligned the proper way. This drawing is solid, but the actual one will consist of various laser cut cross sections.

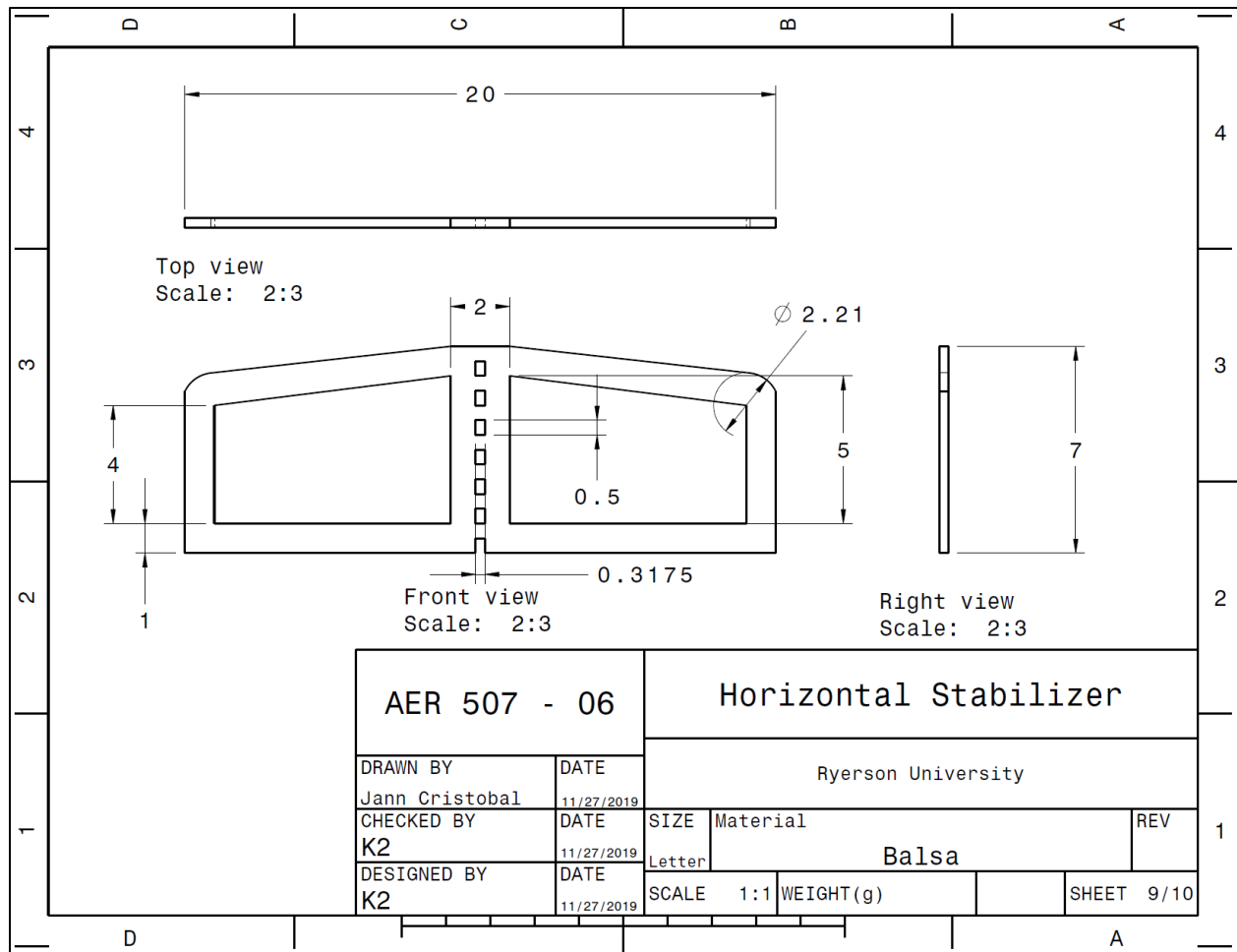


Figure 9.9 – Horizontal Stabilizer

This is the horizontal stabilizer with lighting holes cut-out. These holes serve to reduce the weight of the tail and will be lined with masking tape to still serve its purpose of correcting pitching moment. It will be laser cut from balsa.

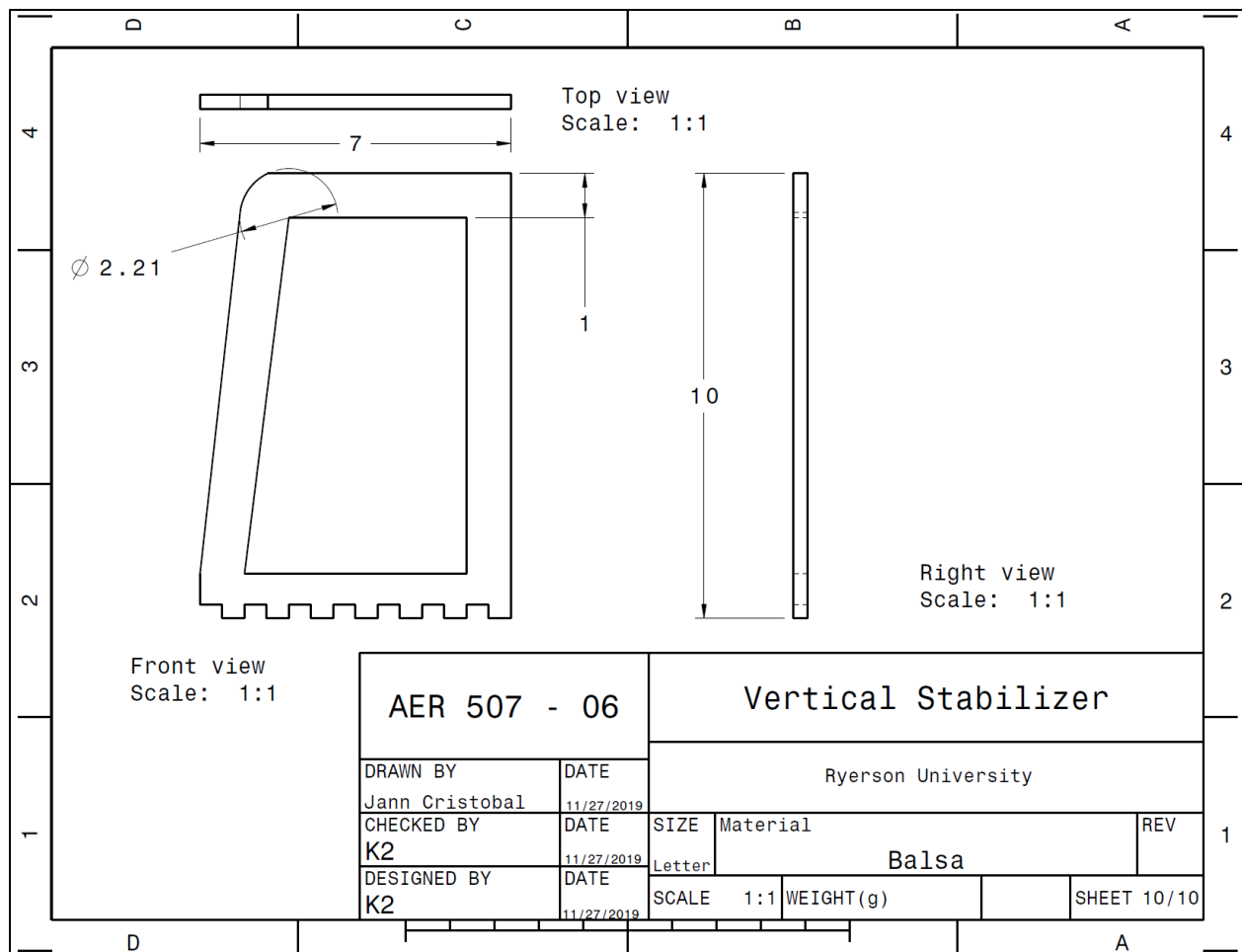


Figure 9.10 – Vertical Stabilizer

This is the vertical stabilizer whose purpose is to correct for the yawing moment. The lightning holes are meant to help reduce the weight and will be lined with masking tape.

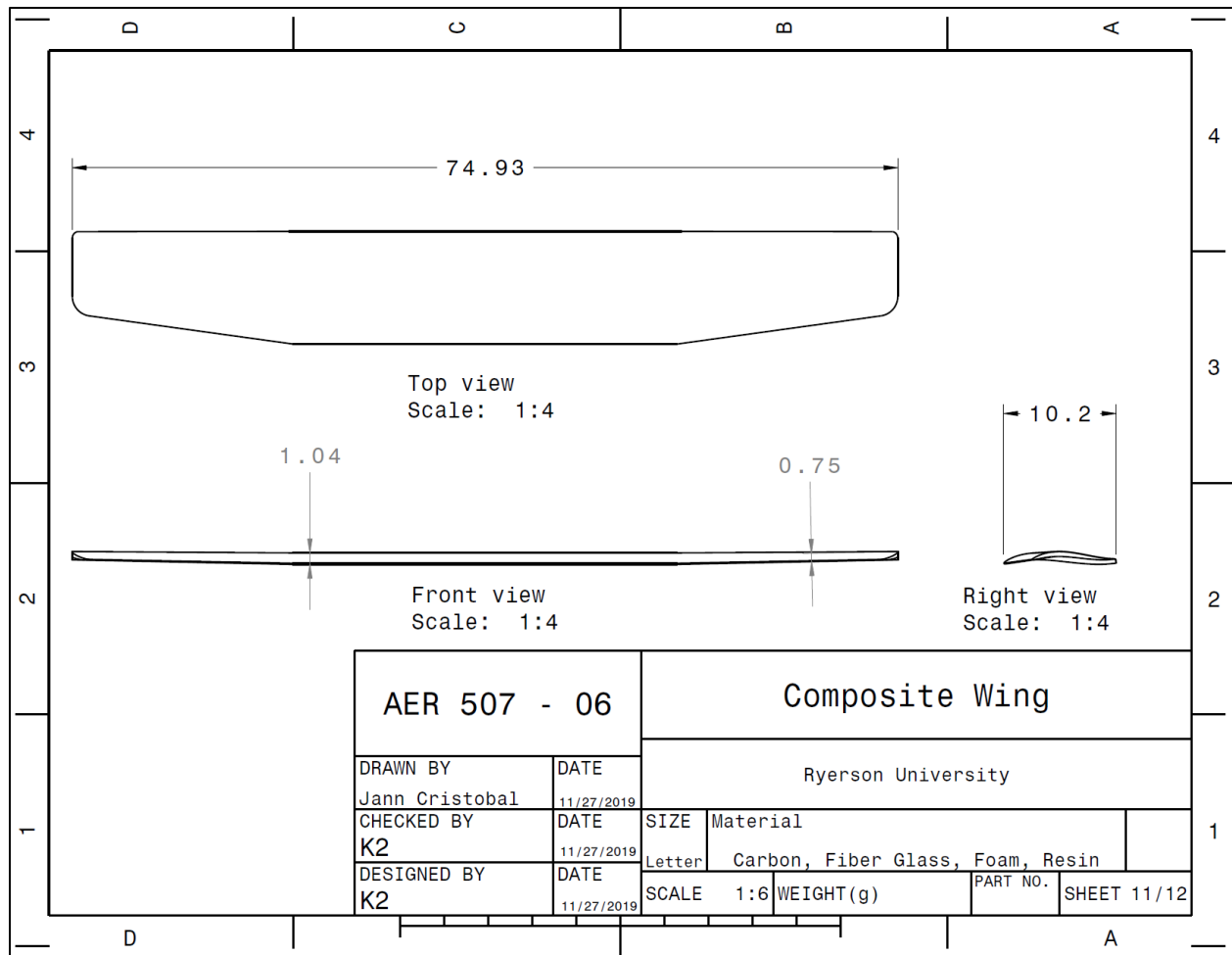


Figure 9.11 – Composite Wing

This is the composite wing that was made during our manufacturing lab. It is made from various materials such carbon, fiber glass, foam and the binding adhesive resin.

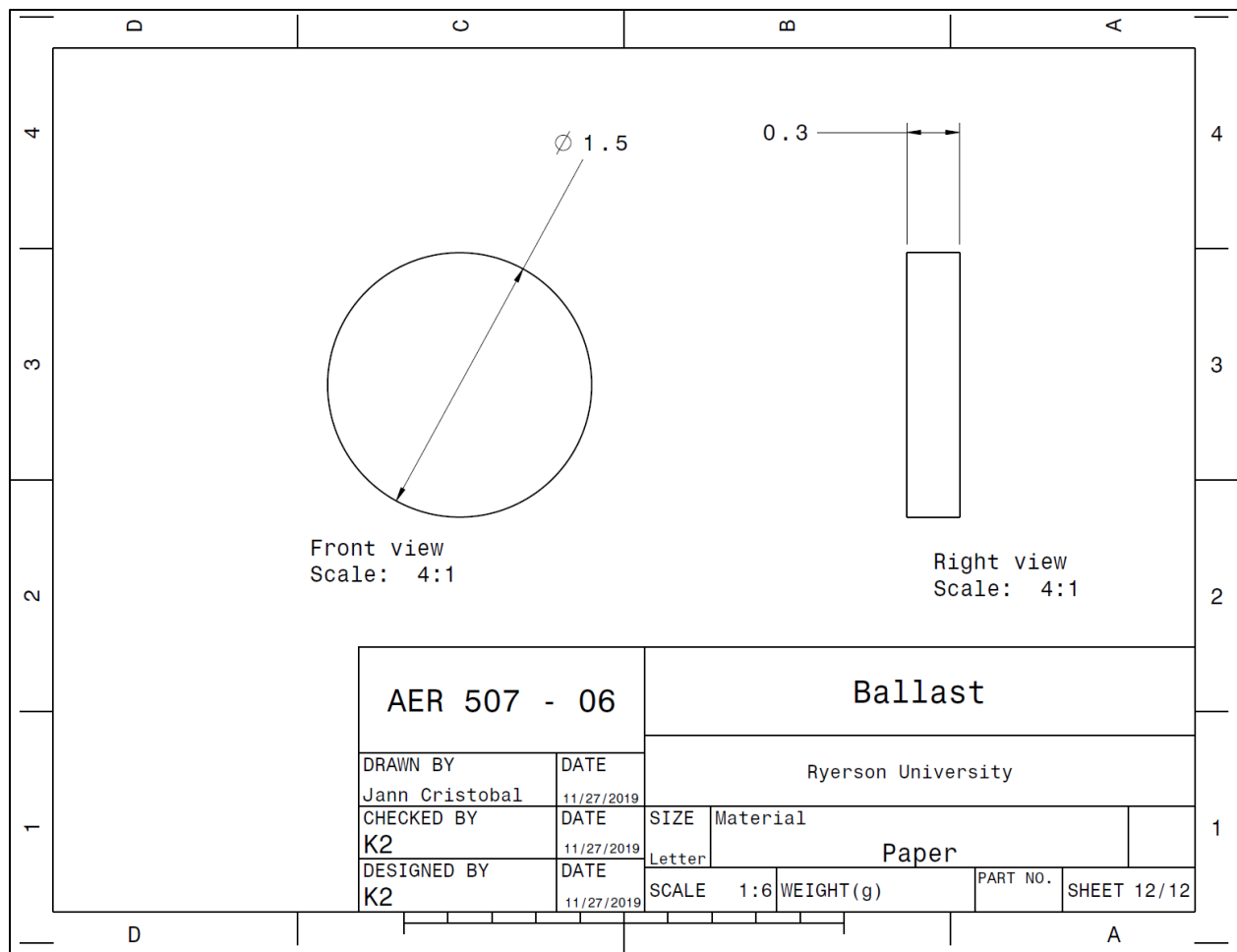


Figure 9.12 – Ballast

This is the counterweight that will be used to balance the glider. The actual shape may vary and even the material used.

Student Name: Jann, Renzo, Pruthvi, Sharjeel				
Lab #:	Section #: 06		TA:	
Component:	Excellent	Good	Needs Improvement	Grade
Introduction				
Formatting				/1.5
Technical Writing				
References				
Procedure				
Formatting				/0.5
Technical Writing				
Results				
Formatting				/0.5
Content				
Calculation				
Formatting				/1.5
Sample Calculations				
Accuracy				
Discussion (Questions)				
Formatting				/3.0
Technical Writing				
Questions				
Conclusion				
Formatting				/3.0
Technical Writing				
Error Analysis				
Conclusion				
Overall:				/10